Machine Learning and Explainable AI for Agricultural Drought Prediction: A Comparative Analysis of Gradient Boosting Methods Using Multi-Source Earth Observation Data

Mirza Md Tasnim Mukarram[1*], Quazi Umme Rukiya[1], Marc Linderman[1], Jun Wang[2,3]

1. School of Earth, Environment, and Sustainability, University of Iowa, IA-52242, Iowa City, Iowa
2. Department of Chemical and Biochemical Engineering, University of Iowa, IA-52242, Iowa City, Iowa
3. Iowa Technology Institute, University of Iowa, IA-52242, Iowa City, Iowa

Corresponding Author*: mtasnimmukarram@uiowa.edu

Abstract

Drought monitoring and prediction remain critical challenges in climate science and agricultural management, particularly under accelerating climate change. This study presents a comprehensive machine learning framework for drought susceptibility mapping in Iowa, USA, using multi-source Earth observation data and explainable artificial intelligence. We systematically evaluated eleven supervised learning algorithms including gradient boosting methods (LightGBM, XGBoost, CatBoost), ensemble approaches (Random Forest, Extra Trees), and neural networks for classifying drought severity based on United States Drought Monitor (USDM) categories. The models were trained on 8,200 stratified samples derived from satellite-based vegetation indices (NDVI, EVI, LAI, FPAR, VCI, VHI), land surface temperature metrics (LST, TCI), precipitation data (CHIRPS), soil moisture (SMAP), and land cover information spanning 2015-2021. Performance evaluation using confusion matrices, F1-scores, and ROC-AUC analysis revealed that gradient boosting algorithms significantly outperformed traditional machine learning approaches, with LightGBM achieving the highest accuracy (95%) and macro-averaged F1-score (0.94). SHAP (SHapley Additive exPlanations) interpretability analysis identified precipitation deficits, soil moisture anomalies, and

vegetation stress as primary drought drivers, with synergistic interactions between elevated temperature and reduced rainfall amplifying severe drought conditions. Spatial predictions demonstrated climatologically consistent patterns, with elevated drought susceptibility in southwestern Iowa and lower risk in northern riverine corridors. The framework's ability to replicate expert-driven drought classifications while providing mechanistic insights establishes machine learning as a viable complement to traditional drought monitoring systems. These findings contribute to the growing body of climate informatics research and provide a transferable methodology for drought early warning systems in agricultural regions globally.

Keywords

Machine Learning; Drought Prediction; Remote Sensing; Explainable Artificial Intelligence; Precision Agriculture Climate Informatics; Earth observation.

1. Introduction

Global temperature rise has accelerated hydroclimatic extremes, making drought one of the most pervasive and consequential natural hazards worldwide. Mean surface temperatures increased by 0.6 °C between 1901 and 2001 (Seo et al., 2025; Pande et al., 2024), intensifying evaporative demand and amplifying water scarcity across diverse climatic zones. Unlike rapid-onset hazards, drought develops gradually over weeks to years (Zhang et al., 2025), exerting prolonged stress on water resources, agricultural productivity, ecosystems, and socio-economic stability (Burka et al., 2024). With global food demand projected to rise by 60–110% by 2050 (Ali et al., 2024), the capacity to assess drought susceptibility (DS) and forecast drought severity has become a crucial component of early warning systems (EWS) and resource planning.

Recent studies highlight sustained intensification of drought frequency, severity, and spatial extent worldwide. Flash droughts are rapidly emerging drought driven by atmospheric evaporative demand (AED) have increased globally nearly 74% over the past six decades (Yuan et al., 2023). Between 2018 and 2022, the global area under moderate to severe drought expanded by nearly 74% relative to 1981-2017, with AED accounting for 42% of the 2022 impacts (Gebrechorkos et al., 2025). Drought accounted for an estimated 650,000 deaths between 1970 and 2019 and more than USD 249 billion damages since 1980 (Mishra et al.,

2025). Approximately 75 million people continue to be directly affected annually (Mani et al., 2024).

In the United States, drought remains one of the most persistent climate-related hazards, disrupting agricultural production, water supply, public health, and regional economies (Leeper et al., 2022)(Leeper et al., 2022; Zhang et al., 2025). National losses since 1980 have exceeded USD 131 billion (Smith,2020). The Midwest, an agricultural hotspot, is particularly vulnerable to drought. Drought-induced rainfall deficits directly reduce yields, disrupt river navigation on the Mississippi and Ohio rivers, and elevate shipping and energy costs (Hoell et al., 2021). The 2012 Midwest drought alone imposed USD 34.5 billion in losses. Future projections anticipate more frequent, prolonged, and severe drought episodes across the central United States (Altman et al.,2024; Kotz et al., 2024).

Effective drought management requires accurate identification of areas most susceptible to drought under evolving climatic, environmental, and land-use conditions. Traditional drought susceptibility mapping (DSM) approaches have not kept pace with the increasing complexity and nonlinearity of drought processes, nor with the expanding volume of remote-sensing (RS) and in-situ environmental data now available for analysis. This underscores the need for advanced technological approaches to address these challenges.

Traditional DSM methods rely heavily on climate indices derived from precipitation and temperature records (Mullapudi et al., 2023). Widely applied indices include the Standardized Precipitation Index (SPI), Palmer Drought Severity Index (PDSI), and Standardized Precipitation Evapotranspiration Index (SPEI), each operating across different temporal scales (Adnan et al., 2023; Keyantash, 2021; Edossa et al., 2016; Vicente-Serrano et al., 2010). Complementary indices such as the Reconnaissance Drought Index (RDI), Effective Drought Index (EDI), Streamflow Drought Index (SDI), Groundwater Resource Index (GRI), agricultural SPI (aSPI), and enhanced Reconnaissance Drought Index (eRDI) have expanded this toolbox (Ahmadi et al., 2021; Deo et al., 2017; Jahangir et al., 2024; Yuce et al., 2023; Katipoğlu, 2023; Azadeh et al., 2025; Sellathurai and Sivakumar, 2021; Tigkas et al., 2022). While the USDM and NDMC (The National Drought Mitigation Center) provide authoritative operational drought monitoring, there remains a methodological need for reproduceable, hig-resolution, and explainable ML frameworks that (i) harmonize multi-sensor predictors, (ii)

systematically benchmark multiple learners under a unified protocol, and (iii) generate sub-county scale drought susceptibility information to support local management decisions. Although these indices quantify hydroclimatic anomalies, they often lack the spatial granularity and non-linear modeling capacity required for fine-scale drought susceptibility assessment. Moreover, linear or rule-based multi-criteria techniques such as Analytical Hierarchy Process (AHP) integrate soil, vegetation, and terrain attributes but cannot robustly capture non-linear relationships or complex interactions that govern DS (Patel and Patel, 2024; Nabiollahi et al., 2024; Abdekareem et al., 2024; Alsafadi et al., 2022).

Studies consistently reported that index-based DSM systems underperform when environmental drivers exhibit nonlinear interactions, abrupt vegetation responses, or threshold behavior (Huang et al., 2025). Statistical drought models such as ARIMA and SARIMA also struggle to represent multi-dimensional environmental predictors and typically require stationary time series (Trion et al.,2021; Hao et al.,2018). As a result, these tools often underestimate DS, misclassify susceptibility zones, or provide delayed warning signals.

Although machine learning (ML) and deep learning (DL) have increasingly been used for drought prediction and mapping, most studies focus on pixel-based predictions or temporal forecasting, with fewer efforts dedicated to producing interpretable and scalable DSM at county and regional levels. Many ML studies also lack systematic benchmarking across architectures, use limited predictor sets, and provide little transparency regarding feature importance, reflecting the black-box nature of ML models. These limitations restrict operational efficiency and hinder effective decision making.

Recent works show that ML models, including RF, CVM, XGBoost, CatBoost, LightGBM, and LSTM, outperform classical statistical models in drought prediction (Xu et al., 2024; Piri et al., 2023; Danandeh et al., 2023; Prodhan et al., 2022). However, these applications often rely on narrow predictor sets, small geographic domains, or short time periods. Interpretability is a major barrier: many ML models function as “black-boxes,” prompting the recent adoption of explainable AI (XAI) tools such as SHAP and LIME to elucidate variable contributions (Samek, 2023; Camps-Valls et al., 2025; Materia et al., 2024). Few studies integrate high-resolution environmental variables with USDM drought categories in a supervised learning framework, and even fewer systematically compare multiple ML algorithms for county-scale.

Iowa is one of the most agriculturally productive states in the U.S. Midwest and faces increasing hydroclimatic stress due to warming temperatures, precipitation variability, and expanding evaporative demand. Its heavy reliance on rainfed agriculture and shallow aquifer systems heightens vulnerability to drought. Yet, DSM research in the Midwest is limited, often conducted at coarse regional scales and lacking fine-scale ML-based susceptibility maps that incorporate USDM classifications. As projections indicate intensifying extremes across the region (Alman et al., 2024), actionable county-level drought risk information is urgently needed to support adaptive water policy, crop planning, and climate-resilient management.

This study addresses these gaps by integrating remote sensing, climate indicators, and advanced ML algorithms to generate a high-resolution DSM for Iowa using USDM severity classifications as the target variable. Eleven ML models- XGBRegressor, CatBoost, LightGBM, Extra Trees, Random Forest (RF), Gaussian Naïve Bayes, K-nearest neighbor, Bagging, Support vector machines (SVM), XGBoost, and Multilayer perceptron are systematically benchmarked. The framework evaluates predictive accuracy, computational performance, and interpretability using SHAP-based XAI to identify the most influential environmental drivers. The novelty lies in (i) the comprehensive comparison of diverse ML algorithms for DSM, (ii) the integration of an explainable, scalable, and replicable ML-XAI workflow tailored to county-scale drought management.

Therefore, the aim of this study is to develop a robust, interpretable, and transferable ML-based methodology for drought susceptibility mapping in Iowa, with potential application to other regions experiencing accelerating hydroclimatic extremes. By combining high-resolution environmental predictors, advanced ML models, and XAI tools, this study contributes an operationally relevant framework for early warning, agricultural planning, and climate-resilient water management.

2. Materials and Methodology

This section outlines the methodological framework adopted in this study, which integrates Earth observation data (EOD) with supervised machine learning (ML) techniques to develop a spatially explicit drought classification system for Iowa. The approach leverages historical drought severity categories provided by the U.S. Drought Monitor (USDM) as reference labels for training. To evaluate temporal generalization, models were trained using annual composites

for 2015-2021 and independently tested on the unseen year 2022. This design provides a forward-year out-of-sample assessments rather than a purely random split. It should be noted that the framework is intended for short-horizon drought classification and susceptibility mapping rather than fully operational seasonal forecasting. Extension to longer lead-time prediction would require the use of strictly antecedent predictors and climate forecast inputs, which is identified as future work. The methodology is structured into seven primary components: study area definition, satellite driven data acquisition, feature engineering, training and validating samples, machine learning model development, accuracy assessment, spatial prediction and visualization of drought risk assessment (**Fig.2**)

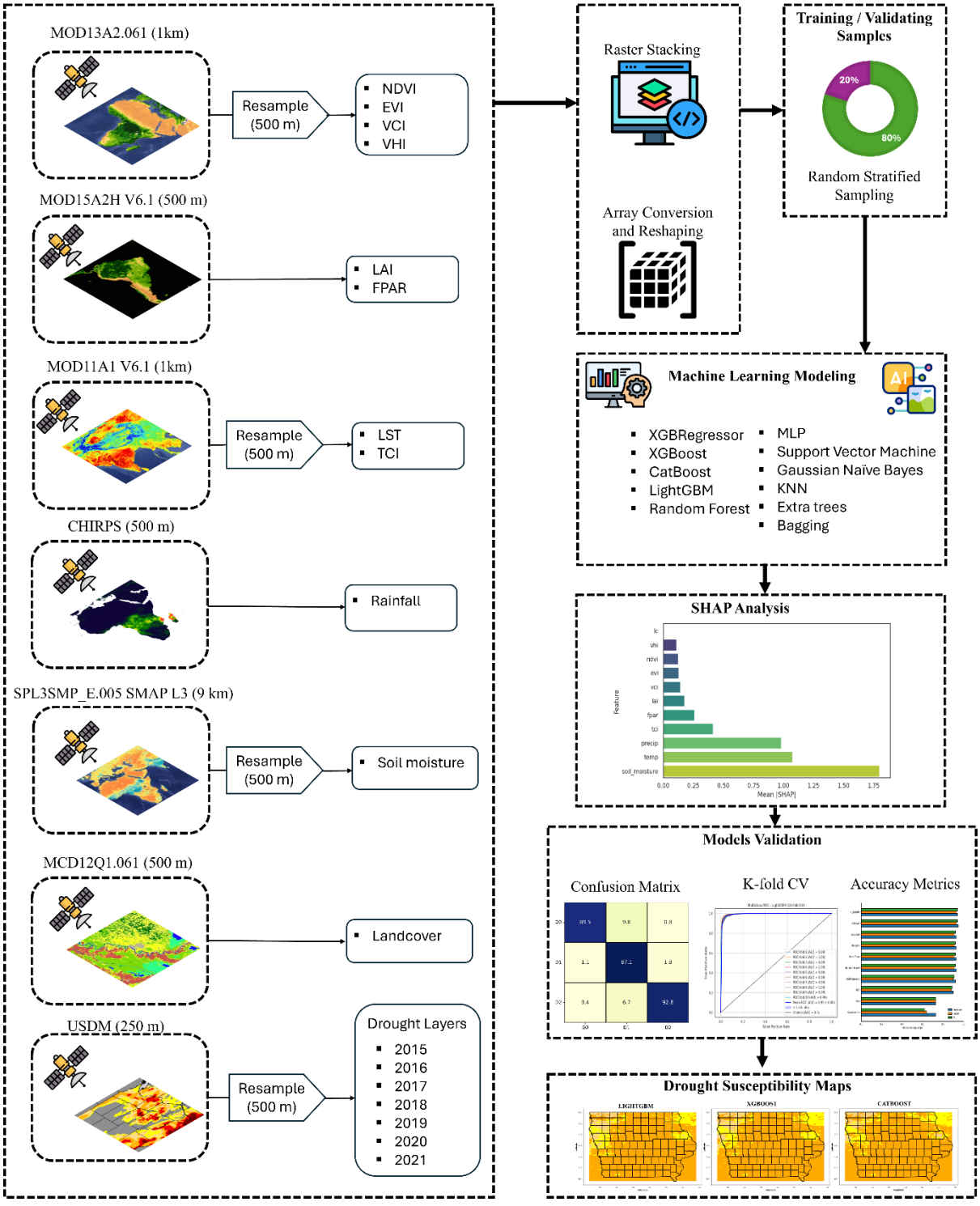

Fig.2 Methodology flowchart for this study

2.1 Study Area

Iowa is located in the heart of the American Midwest, extends between 40°23′ and 43°30′ North latitude and 90°8′ and 96°38′ West longitude (Islam et al.,2025), covering an area of about 145,743 square kilometers (**Fig.3**). The state is bounded by two of the most important river systems in North America: the Mississippi River forms its eastern border, while the Missouri and Big Sioux Rivers define much of its western edge (Shepard et al.,2024). Within the state, a dense network of rivers and tributaries (Yang and Jin,2010) including the Des Moines, Cedar, Iowa, Skunk, and Raccoon Rivers, drains into either the Mississippi or Missouri basins, creating a landscape that is both hydrologically interconnected and sensitive to climate variability (Yildirim and Demir,2022). The physiography of Iowa is shaped by repeated glaciations that produced gently rolling plains, fertile loess soils, and extensive agricultural landscapes. Over 85 percent of the land area is under cultivation, with corn and soybeans dominating the cropping system (USDA,2024, Cintura and Arenas,2025). The state consistently ranks as the leading U.S. producer of corn and ethanol, while also contributing significantly to soybean, pork, and egg production (Sun et al.,2025; Peters, 2024). This agricultural prominence makes Iowa highly vulnerable to fluctuations in water availability (Grant et al.,2024). Even short-term precipitation deficits can reduce moisture, lower crop yields, and cause cascading impacts on regional and global commodity markets.

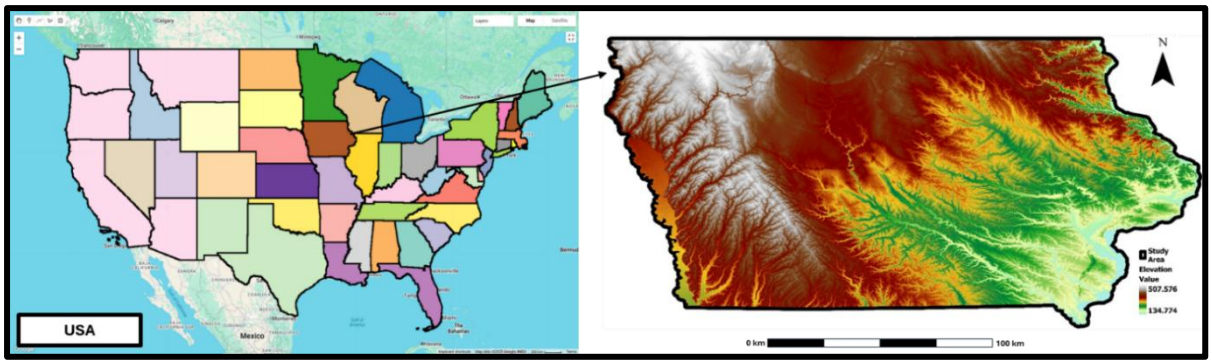

Fig.3 Location of study area with DEM map

Iowa has a humid continental climate with marked seasonality (Hashemi et al.,2025). Average annual precipitation during agricultural production ranges from approximately 400 mm to 600 mm (Islam et al.,2025). Average annual temperatures vary from about 7 °C in the north to 11 °C in the south. Summers are warm to hot and often humid, while winters are cold, with frequent snowfall. Precipitation patterns and temperature variability are strongly influenced by

large-scale atmospheric phenomena such as the El Niño–Southern Oscillation, which can lead to either wetter or drier than normal conditions.

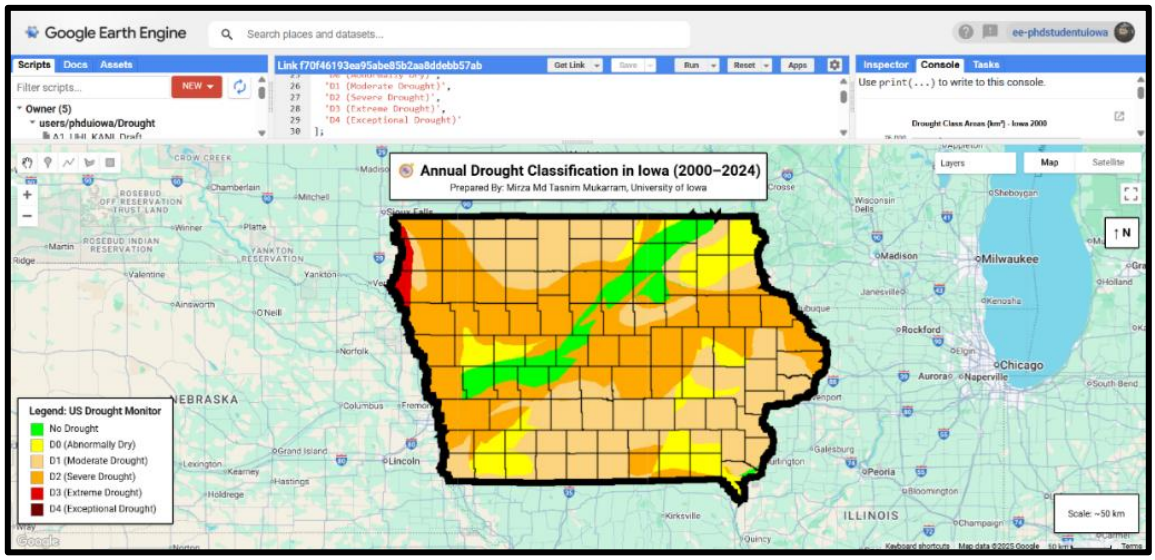

Fig.4 United States Drought Monitor annual classification for Iowa in 2012 showing spatial variability in drought severity across the state.

From a climate risk perspective, Iowa represents a critical case study. Iowa has incurred substantial drought and flood damage across both its urban centers and agricultural regions. From 1980 to 2024, Iowa experienced 16 drought-related disaster events with individual damages exceeding USD 1 billion (NOAA,2024) and since 1953, the state has recorded 29 federally declared flood disasters (Yildirim and Demir,2022; FEMA,2021). It is simultaneously a global center of agricultural production and a region increasingly exposed to climate extremes. **Fig.4** shows an illustration of USDM based drought of 2012 in Iowa. Projections indicate that rising evapotranspiration and shifting precipitation regimes will intensify drought frequency and severity in the Midwest, making Iowa an ideal laboratory for advancing drought susceptibility mapping and predictive modeling.

2.2 Satellite data acquisition

The predictor dataset integrated twelve drought-influencing variables (Table 1), derived from Earth observation and reanalysis products and accessed primarily through Google Earth Engine (GEE) and complementary repositories. The temporal coverage extended from 2015 to 2021, capturing interannual hydroclimatic variability across Iowa. Spatial resolutions varied

substantially, from 500 m for MODIS-derived vegetation metrics (LAI, FPAR) to 9 km for SMAP soil moisture, while temporal frequencies ranged from 8-day (vegetation, temperature, and moisture indices) to annual land cover composites. All variables were resampled and harmonized to a uniform 0.05° (~5 km) grid and reprojected to the NAD 1983 coordinate system to ensure cross-variable comparability (Glinka et al., 2022).

The feature set encompassed vegetation indices (NDVI, EVI, LAI, FPAR, VCI, VHI), thermal condition proxies (LST, TCI), and hydroclimatic drivers including precipitation (CHIRPS) and volumetric soil moisture (SMAP, 9 km, 2–3-day composites). Land cover information (MCD12Q1, 500 m, annual) provided structural context, while USDM-based categorical drought layers (0.025°, weekly) served as the ground-truth inventory for supervised classification. Preprocessing involved rescaling variables using sensor-specific scaling factors, aggregating to annual composites to minimize short-term variability, and excluding pixels with missing values. The resulting geospatial stack constituted a consistent, multivariate dataset suitable for training and validation of supervised machine learning classifiers, accuracy assessment, and subsequent drought susceptibility mapping.

2.3 Feature preparation

2.3.1 Drought inventory preparation

The drought inventory in this study was derived from the U.S. Drought Monitor (USDM), which integrates various drought indicators such as precipitation anomalies, soil moisture, vegetation indices, and expert assessments (Hobeichi et al.,2022). These factors are used to classify drought severity into a five-class ordinal scale, ranging from D0 (abnormally dry) to D4 (exceptional drought) (Svoboda et al., 2002). The drought inventory serves as a consistent, operational benchmark for drought monitoring and has been previously employed in machine learning studies replicating USDM classifications (Hatami et al., 2021). The annual USDM composite classifications were accessed via Google Earth Engine (GEE) and rasterized onto the study grid at a resolution of 0.05°. These categorical historical drought layers of study area were used as the ground truth for training the predictive model. By intersecting the layers, the final image was taken which filtered only those pixels common in all the seven drought events. For sampling a total of 8200 samples were generated using equally random stratified techniques

(Waleed and Sajjad, 2025) ensuring balanced proportions for each drought class. Then, all the samples were split into 80% for training and 20% for testing the ML models.

2.3.1.1 Drought Classification Labels

The target variable in this study was derived from the United States Drought Monitor (USDM), a nationally integrated drought classification system (Hatami et al., 2021; Cintura & Arenas, 2025). The USDM assigns drought severity on a five-category ordinal scale, ranging from D0 (Abnormally Dry) to D4 (Exceptional Drought), based on a convergence of indicators, including precipitation anomalies, vegetation health, soil moisture deficits, and expert interpretations. The classification is updated weekly and reflects a consensus drawn from both quantitative datasets and field-level assessments.

In this study, annual USDM composite rasters were obtained via Google Earth Engine (GEE) and restructured into categorical formats to serve as the ground truth for training and validating the supervised drought classification model. This process ensures that the dataset captures the full variability and complexity of drought severity across the study region.

To highlight the robustness and suitability of the USDM for machine learning applications, **Table 2** summarizes the key structural and operational features of the USDM, which makes it a widely trusted source for understanding drought conditions across the U.S. and globally.

Table 2. Structural and operational features of the United States Drought Monitor (Hatami et al.,2021; Svoboda et al.,2002)

Characteristic	**Description**
Nationwide Integration	Coordinated by the NDMC, USDA, CPC, and NCEI, with authors rotating biweekly to produce updated maps.
Local Expert Collaboration	Involves input from over 425 field observers (e.g., climatologists, hydrologists, USDA officials) who contribute regional knowledge to refine classifications.
Simplicity and Transparency	The D0–D4 classification scale is easily interpretable and widely adopted in policy and communication contexts.

Multivariate Integration	Synthesizes diverse data including precipitation, soil moisture, streamflow, vegetation stress, and remote sensing products.
Flexible and Adaptive	Continuously integrates new technologies and data streams to maintain scientific rigor and operational relevance.
Timely and Consistent	Released weekly, the maps provide up-to-date drought conditions and facilitate near-real-time decision-making.

2.3.2 Drought Conditioning Factors

A recent study by Burka et al.,2024 used 15 drought influencing factors but, in this study, we used 11 factors (**Fig.5**) depending on the ease of data availability and speed of ML model processing. In this study the multivariate feature set was designed to capture biophysical and hydroclimatic processes relevant to drought (Hao and Singh, 2015). This included vegetation greenness and canopy structure (NDVI, EVI, LAI, FPAR), (Ma et al.,2023) surface thermal dynamics (LST, TCI) (Li et al.,2024; Lu et al.,2013), moisture availability (precipitation, soil moisture) (Oyounalsoud et al.,2024), and land cover (Xiao et al.,2023). Additional indices such as the Vegetation Condition Index (VCI) and the Vegetation Health Index (VHI) were derived by integrating vegetation stress with thermal anomalies (Kogan,1995), thereby enhancing sensitivity to drought impacts on ecosystems (Bento et al.,2018).

2.3.3 Data preparation and preprocessing for drought variables

To construct a consistent, scalable, and geospatially robust input dataset for drought modeling, we synthesized a multi-source stack of remote sensing variables over the state of Iowa. Leveraging Google Earth Engine (GEE) as the primary data platform, we accessed harmonized Earth observation products spanning vegetation dynamics (MODIS MOD13A2 and MOD15A2H), thermal regimes (MOD11A2), hydrometeorological indices (CHIRPS precipitation, SMAP soil moisture), and land surface classifications (MCD12Q1). The raw imagery was aggregated temporally (mean composites for 2015–2021), then spatially subset to Iowa's administrative boundary using the TIGER 2018 shapefile (U.S. Census Bureau, 2018). Each raster variable was rescaled using standard factors documented in MODIS technical guides—e.g., NDVI and EVI by 0.0001, LST by 0.02, and LAI/FPAR by 0.1. Additional condition indices were derived to enhance vegetation–climate interaction modeling: the

Temperature Condition Index (TCI) and Vegetation Condition Index (VCI) were calculated via min-max normalization of LST and NDVI, respectively. These two indices were further integrated into the Vegetation Health Index (VHI), aligning with prior drought impact studies (Kogan, 1997; Hao & AghaKouchak, 2014). The resulting variables were compiled into a single 12-band georeferenced composite image (including the drought training image) and converted into a 3D xarray.Dataset, facilitating efficient memory handling and array-based operations over large spatiotemporal domains (Hoyer & Hamman, 2017). Using the xee engine, this raster stack was extracted to a tabular format (pandas.DataFrame) via pixel-level flattening, enabling subsequent machine learning workflows. **Figure 6** illustrates the preprocessing pipeline, where satellite-derived variables were transformed from raw multi-band rasters into spatially consistent arrays and ultimately into a structured 2D tabular format. This progression—from pixel to dataframe—ensures interoperability across Python's scientific computing ecosystem (e.g., scikit-learn, xgboost, SHAP). Moreover, such integration aligns with best practices in replicating the U.S. Drought Monitor (USDM) categories (Hatami et al., 2021; Cintura & Arenas, 2025), while supporting reproducibility through open-access data sources and scalable cloud-based processing.

By aggregating vegetation health, land surface characteristics, thermal anomalies, and moisture availability, the data preprocessing stage provides a holistic representation of drought-relevant phenomena. This multivariate conditioning ensures that downstream classification models can capture the nonlinear interactions among agro-ecological and climatological variables, thereby enhancing predictive performance and policy relevance.

Table 1. Data types, sources and related attributes of data used in this research

No.	Parameters	Data Type	Resolution	Data Provider	Source (Data Extraction Website)	Temporal Window
1	NDVI	Satellite-derived index that measures the density of chlorophyll (greenness)	1 km, 16-day composites	U.S. Geological Survey (USGS) Earth Resources Observation and Science (EROS) Center (MOD13A2.061)	https://www.chc.ucsb.edu/	2015-2021
2	EVI	Enhanced vegetation index	1 km, 16-day composites	U.S. Geological Survey (USGS) Earth Resources Observation and Science (EROS) Center	https://www.chc.ucsb.edu/	2015-2021
3	Fpar	Fraction of Photosynthetically Active Radiation	500 m, 8-day composites	NASA MODIS (MOD15A2H)	https://www.earthdata.nasa.gov/centers/lp-daac	2015-2021
4	LAI	Leaf Area Index	500 m, 8-day composites	NASA MODIS (MOD15A2H)	https://www.earthdata.nasa.gov/centers/lp-daac	2015-2021
5	TCI	Temperature Condition Index	1 km, 8-day composites	NASA MODIS (MOD11A2 LST product)	https://www.earthdata.nasa.gov/centers/lp-daac	2015-2021
6	LST	MODIS LST	1 km, 8-day composites	U.S. Geological Survey (USGS) Earth Resources Observation and Science (EROS) Cente	https://earlywarning.usgs.gov/	2015-2021
7	VCI	Vegetation Condition Index	1 km, 8-day composites	NASA MODIS (derived index)	https://www.earthdata.nasa.gov/centers/lp-daac	2015-2021
8	VHI	Vegetation Health Index (blended from VCI and TCI)	1 km, 8-day composites	National Integrated Drought Information System (NIDIS)	https://cpo.noaa.gov/	2015-2021
9	Precipitation	CHIRPS rainfall	0.05°, daily aggregates	University of California, Santa Barbara (UCSB) & U.S. Geological Survey (USGS)	https://chc.ucsb.edu/data/chirps	2015-2021
10	Soil moisture	Volumetric water content (%)	9 km, 2-3 days	SPL3SMP_E.005 SMAP L3 Radiometer Global Daily	https://nsidc.org/data/spl3smp_e/versions/5	2015-2021
11	Land cover	Land Use and Land Cover (Sentinel-2 / ESRI Living Atlas)	500 m, annual	MCD12Q1, Version 6.1	https://earthengine.google.com/	2015-2021
12	Drought layers		0.025°, weekly	National Drought Mitigation Center,USDA, NOAA	https://droughtmonitor.unl.edu/	2015-2021

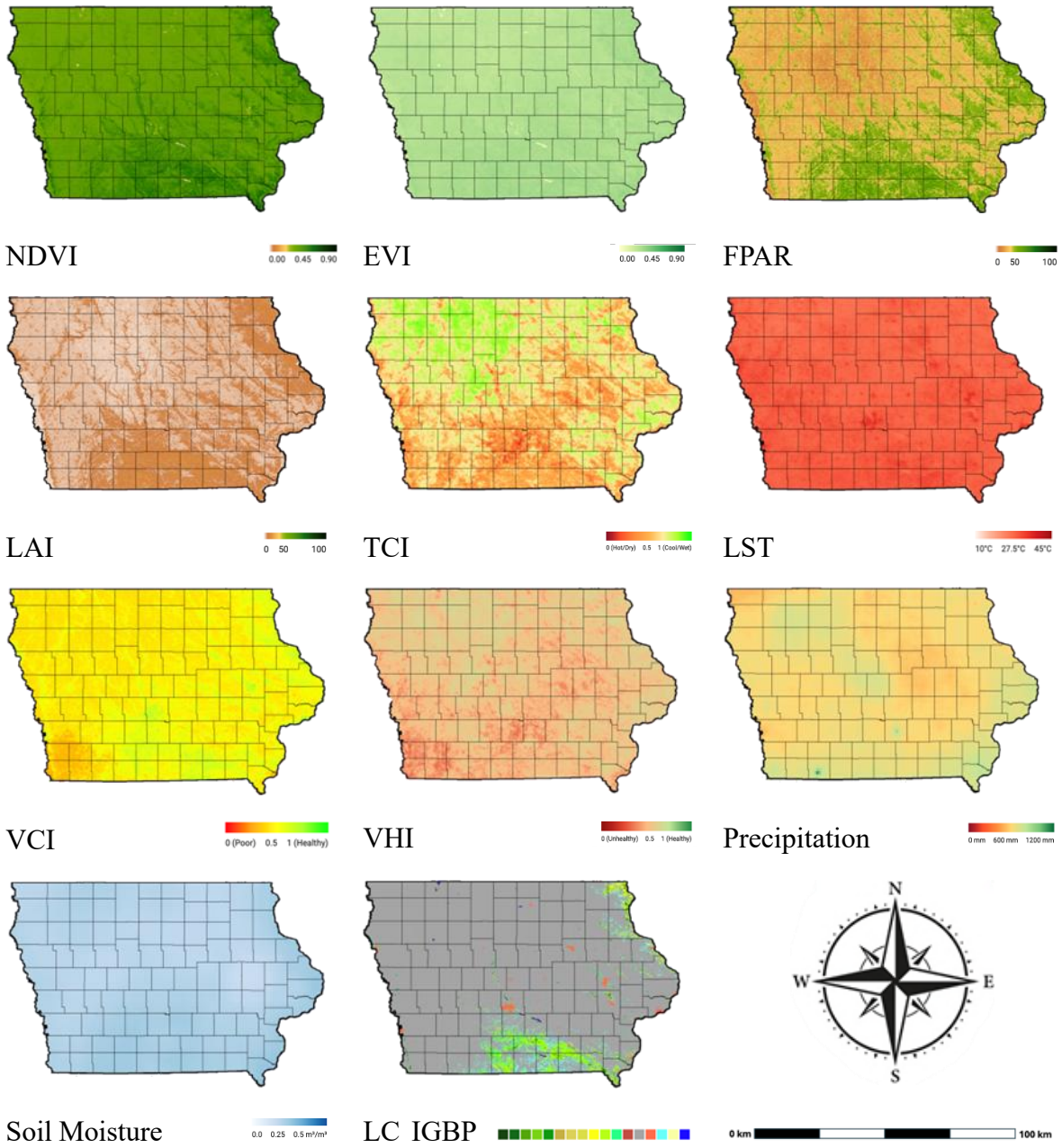

Figure 5. Drought influencing factors (NDVI, EVI, FPAR, LAI, TCI, LST, VCI, VHI, Precipitation, Soil Moisture, and Land Cover).

(a)

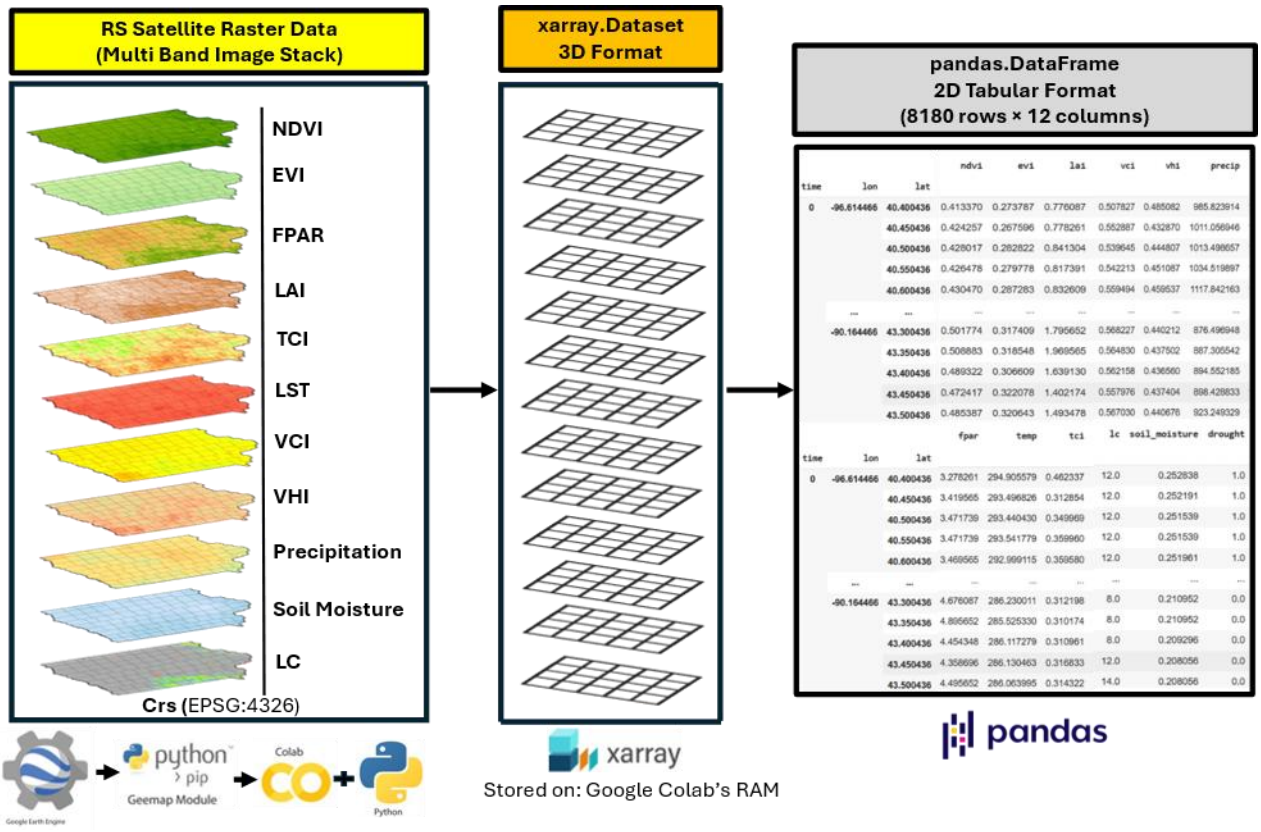

(b)

time	lon	lat	ndvi	evi	lai	vci	vhi	precip
0	-96.614466	40.400436	0.413370	0.273787	0.776087	0.507827	0.485082	985.823914
		40.450436	0.424257	0.267596	0.778261	0.552887	0.432870	1011.056946
		40.500436	0.428017	0.282822	0.841304	0.539645	0.444807	1013.496657
		40.550436	0.426478	0.279778	0.817391	0.542213	0.451087	1034.519897
		40.600436	0.430470	0.287283	0.832609	0.559494	0.459537	1117.842163
...	...	...	...	...	...	...	...	...
	-90.164466	43.300436	0.501774	0.317409	1.795652	0.568227	0.440212	876.496948
		43.350436	0.506883	0.318548	1.969565	0.564830	0.437502	887.306542
		43.400436	0.489322	0.306609	1.639130	0.562158	0.436560	894.552185
		43.450436	0.472417	0.322078	1.402174	0.557976	0.437404	898.428833
		43.500436	0.485387	0.320643	1.493478	0.567030	0.440676	923.249329

time	lon	lat	fpar	temp	tci	lc	soil_moisture	drought
0	-96.614466	40.400436	3.278261	294.905579	0.462337	12.0	0.252838	1.0
		40.450436	3.419565	293.496826	0.312854	12.0	0.252191	1.0
		40.500436	3.471739	293.440430	0.349969	12.0	0.251539	1.0
		40.550436	3.471739	293.541779	0.359960	12.0	0.251539	1.0
		40.600436	3.469565	292.999115	0.359580	12.0	0.251961	1.0
...	...	...	...	...	...	...	...	...
	-90.164466	43.300436	4.676087	286.230011	0.312198	8.0	0.210952	0.0
		43.350436	4.895652	285.525330	0.310174	8.0	0.210952	0.0
		43.400436	4.454348	286.117279	0.310961	8.0	0.209296	0.0
		43.450436	4.356696	286.130463	0.316833	12.0	0.208056	0.0
		43.500436	4.495652	286.063965	0.314322	14.0	0.208056	0.0

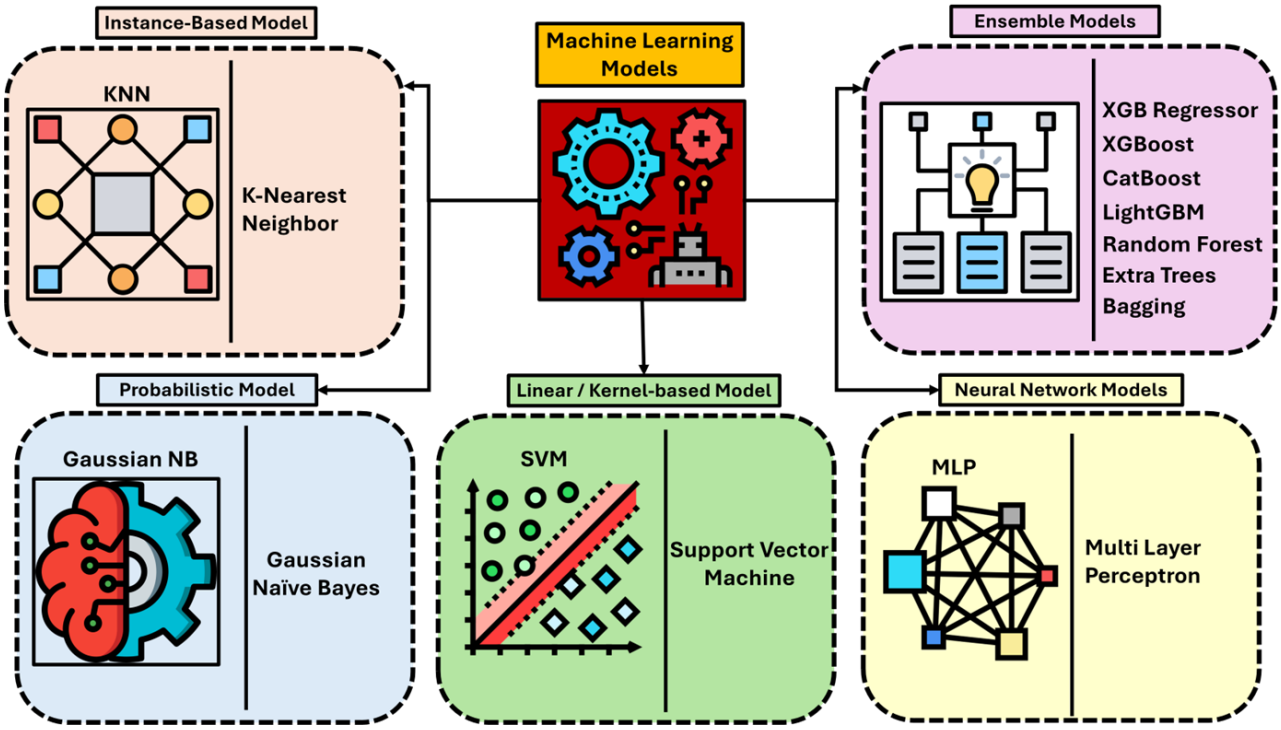

Fig.6 (a) Feature conversion process (b) Different categories of ML models used in this study

2.4 ML Model Validation

To evaluate categorical performance, confusion matrices were constructed, from which overall accuracy, precision, recall, and F1-scores were derived. Receiver Operating Characteristic (ROC) curves and their corresponding Area Under the Curve (AUC) values were also generated to examine the capacity of the models to discriminate between drought categories.

The use of these complementary metrics allowed evaluation of both model fit and classification ability, thereby ensuring that predictive performance was assessed across multiple dimensions relevant to drought forecasting. A summary of the accuracy metrics, their equations, and justifications is provided in **Table 3**.

Table 3. Accuracy assessment metrics used in this study

Name	Description	Equation	Justification
Accuracy	Proportion of correctly classified drought categories among all predictions.	$Accuracy = \frac{TP + TN}{TP + TN + FP + FN}$	Hobeichi et al.,2022

Precision	Fraction of correctly predicted drought cases among all cases predicted as drought.	$Precision = \frac{TP}{TP + FP}$	Melese et al.,2025
Recall	Fraction of actual drought cases correctly identified by the model.	$Recall = \frac{TP}{TP + FN}$	Ali et al.,2024
F1-score	Harmonic means precision and recall.	$F_1 = \frac{2 \cdot Precision \cdot Recall}{Precision + Recall}$	Barradas et al.,2021
ROC–AUC	Area under the ROC curve summarizing model discrimination ability across thresholds.	The ROC curve is constructed by plotting the true positive rate (TPR) against the false positive rate (FPR) at different classification thresholds	Zhang et al.,2023

Abbreviations: TP, true positives (correctly predicted drought cases); TN, true negatives (correctly predicted non-drought cases); FP, false positives (model predicted drought where none existed); FN, false negatives (model missed actual drought); N, total number of instances;y, observed U.S. Drought Monitor (USDM) drought category;$\hat{y}$,predicted drought category. For multi-class classification (D0–D4), TP, TN, FP, and FN were computed for each category using a one-vs-all framework.

4.Results

4.1 Models Validation

The predictive capacity of eleven supervised machine learning algorithms was assessed across three drought severity categories defined by the U.S. Drought Monitor (USDM): D0 (abnormally dry), D1 (moderate drought), and D2 (severe drought). These categories were treated as ordinal targets, with pronounced class imbalance (D0 = 256, D1 = 934, D2 = 446). To mitigate skewed influence from majority classes, evaluation relied on macro-averaged F1-scores alongside overall accuracy, ensuring equitable representation of minority classes. Class-specific F1-scores are displayed in **Figure 7**, while macro-averaged metrics and aggregate accuracies are summarized in **Figure 8**. Comparative breakdowns of precision, recall, and F1 across all algorithms are presented in **Figure 9**.

Ensemble gradient boosting methods emerged as the most robust classifiers. LightGBM achieved the highest overall accuracy (0.95) and consistently high F1-scores across all classes: 0.91 (D0), 0.96 (D1), and 0.94 (D2). XGBoost yielded nearly identical results, with particularly

strong discrimination of D2, the class most relevant to operational drought early warning. CatBoost demonstrated comparable generalization, though with a marginal decline in precision for D0, reflecting the limited sample size and greater spectral–climatic heterogeneity of this category. These findings align with recent literature emphasizing the superior adaptability of gradient boosting to nonlinear, multivariate hydrometeorological data (Díaz-Ramírez et al., 2024; Li et al., 2025).

By contrast, non-ensemble learners such as K-Nearest Neighbors (KNN) and Gaussian Naïve Bayes (GNB) showed limited effectiveness, with macro F1-scores of 0.73 and 0.62, respectively. Their misclassification patterns were most acute for D0, highlighting structural deficiencies in modeling the subtle hydroclimatic transitions between near-normal and abnormally dry conditions. These deficiencies underscore the limited capacity of distance-based or probabilistic learners to capture the nonlinear drought signatures embedded in high-dimensional remote sensing and reanalysis datasets (Halder et al., 2024).

Visual comparisons reinforce these conclusions. **Figure 7** illustrates that boosting algorithms maintain superior recall and precision across all severity categories, particularly stabilizing performance in minority classes. **Figure 8a** demonstrates the elevated macro-F1 of ensemble methods relative to baselines, while **Figure 8b** confirms their accuracy advantage. **Figure 9** extends this view by jointly examining precision, recall, and F1, showing the structural superiority of boosting models across the entire drought spectrum.

Collectively, these findings establish ensemble gradient boosting algorithms as the most reliable tools for drought classification in data-rich but climatically heterogeneous regions such as Iowa. Their ability to maintain predictive accuracy across both minority and majority classes strengthens their candidacy for integration into operational drought monitoring systems, complementing the expert-driven framework of the USDM and enhancing early warning capabilities (Wang et al., 2025; Zhang et al., 2025)

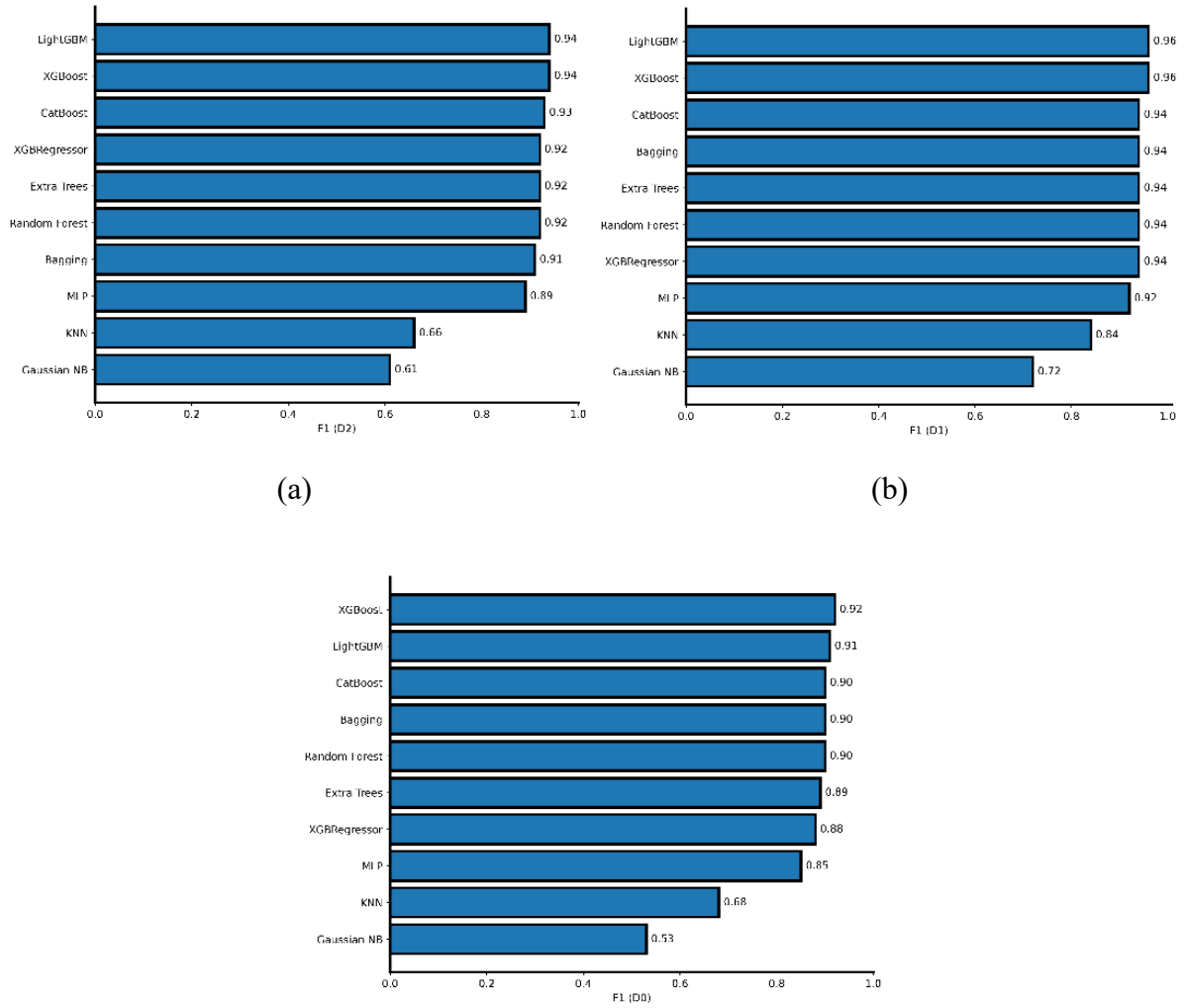

Fig. 7 Class-wise F1-scores of machine learning algorithms for drought classification: (a) Abnormally Dry (D0), (b) moderate drought (D1), and (c) severe drought (D2).

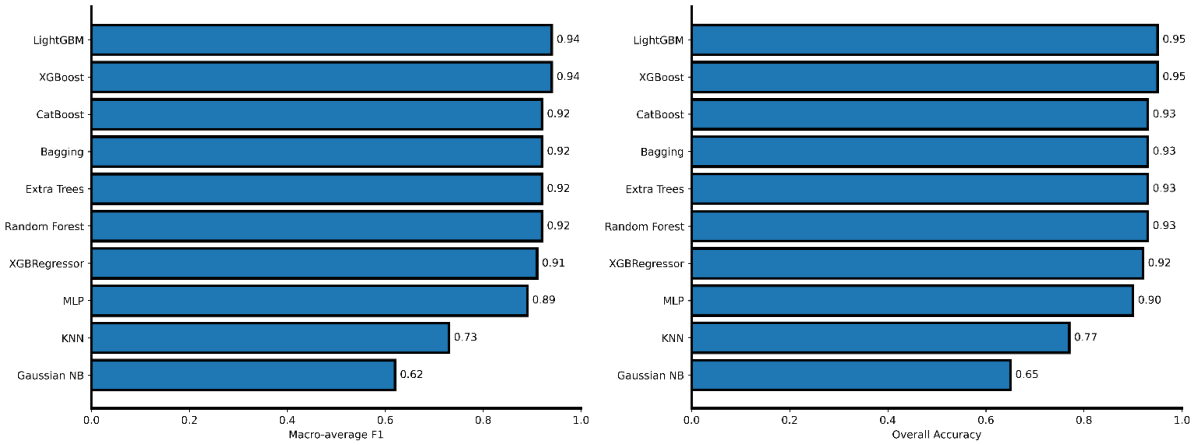

(a) (b)

Fig.8 Macro-average F1(a) and overall accuracy (b) of machine learning models applied to drought prediction, highlighting relative strengths across classifiers.

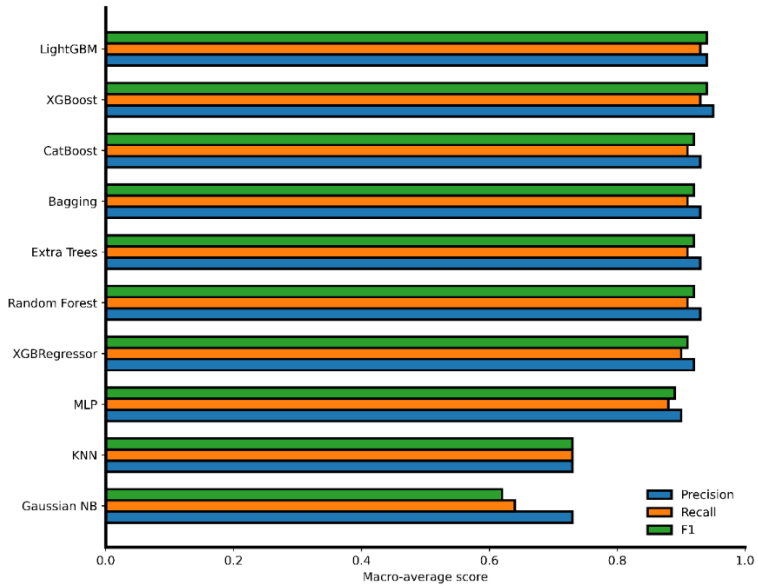

Fig.9 Comparative precision, recall, and F1-scores of eleven machine learning algorithms for drought classification (D0–D2)

4.2 Comparison of Machine Learning Models

Confusion matrices and ROC-AUC diagnostics (**Figures 10 and 11**) were used to probe classification reliability across the three drought categories. LightGBM and XGBoost achieved the lowest misclassification rates, with true positive rates exceeding 93% for D1 and D2, and minimal leakage across adjacent classes. LightGBM misclassified only 4.7% of D0 samples as drought, reflecting a particularly low false-alarm rate, while XGBoost displayed enhanced sensitivity to D2, the most operationally critical category in drought surveillance. CatBoost, although marginally less stable, outperformed all non-ensemble baselines by maintaining high recall for D1.

Tree-based ensemble methods such as Random Forest and Extra Trees achieved competitive aggregate accuracy, yet their confusion matrices revealed higher D0–D1 ambiguity, confirming their tendency to blur class boundaries under imbalanced distributions. Neural models such as the multilayer perceptron (MLP) produced balanced results overall but disproportionately misclassified D0, reflecting the structural difficulty of detecting subtle deviations from normal

conditions. Simpler classifiers, notably Gaussian Naïve Bayes and K-Nearest Neighbors, exhibited diagnostic unreliability: GNB misclassified over 30% of D0 cases as drought, while KNN displayed heightened sensitivity to noise, underscoring their unsuitability for operational deployment.

ROC-AUC curves (**Figure 11**) corroborated these findings. Boosting-based models yielded steep, high-AUC profiles with minimal variance across iterations, highlighting robust probabilistic separability. In contrast, GNB and KNN trajectories approached random baselines, confirming their limited discriminative power. These results collectively establish gradient boosting algorithms as the most consistent classifiers for drought severity mapping, corroborating recent comparative studies in environmental machine learning (Díaz-Ramírez et al., 2024; Li et al., 2025).

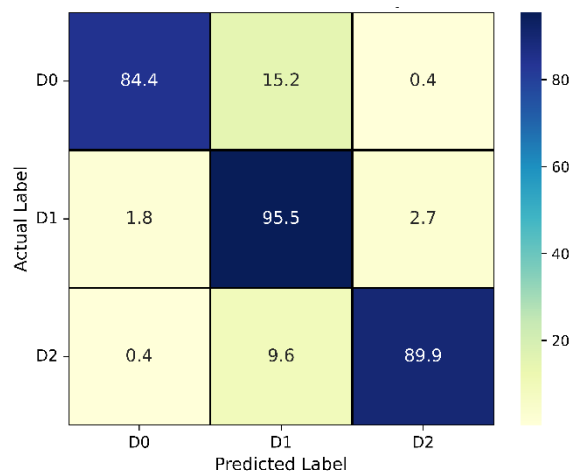

XGB Regressor

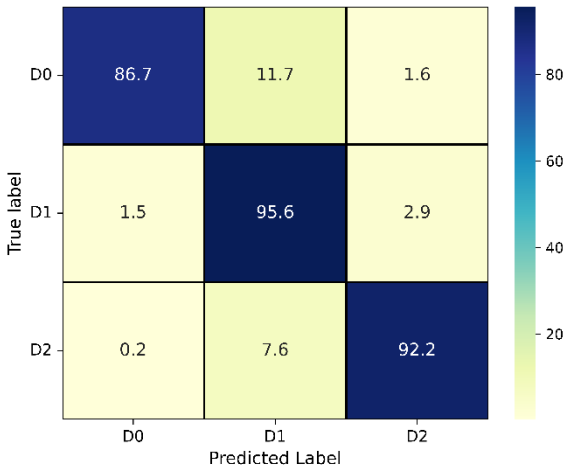

Cat Boost

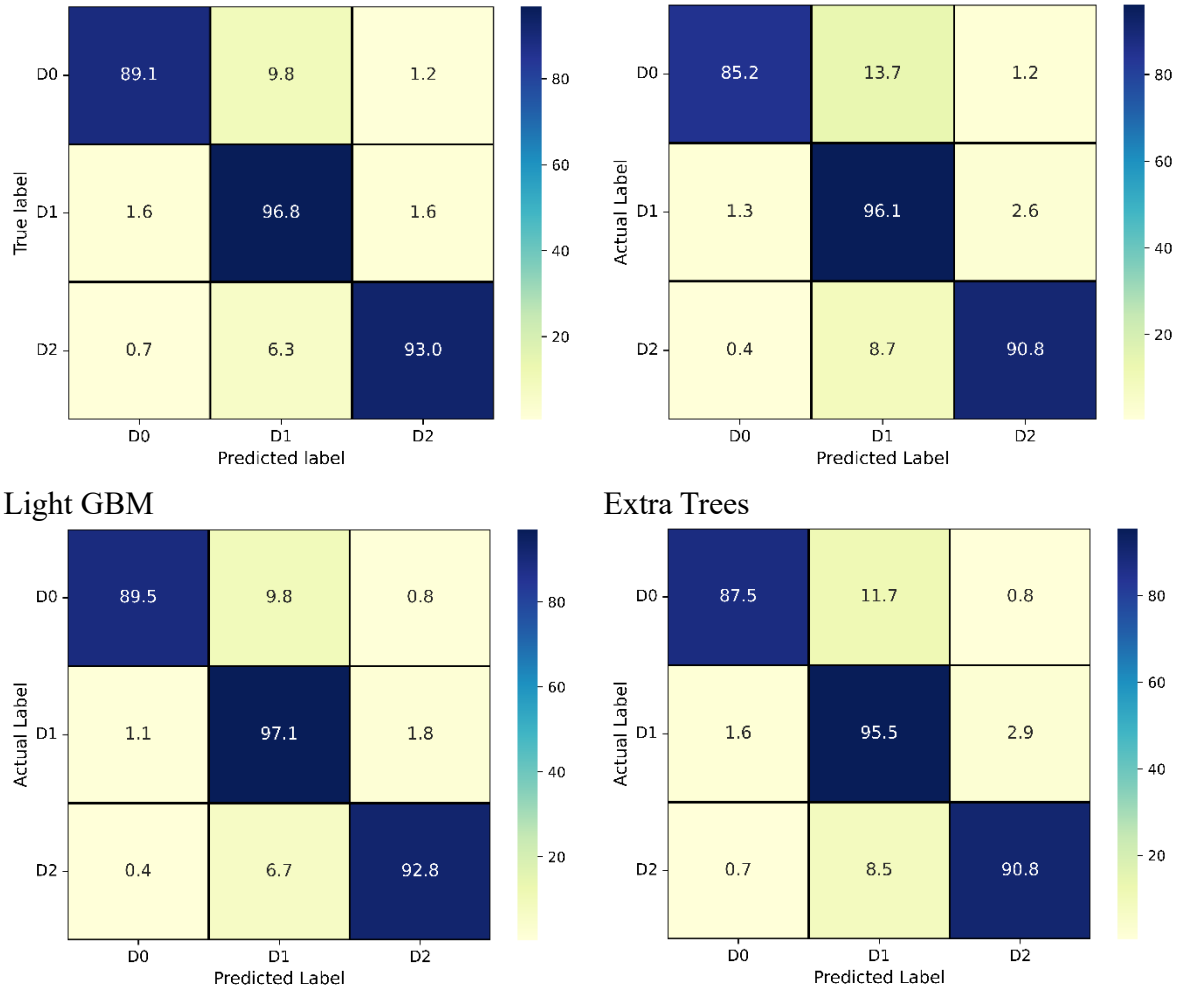

Fig.10 Confusion matrices of predicted drought classes (D0: Abnormally Dry, D1: Moderate Drought, D2: Severe Drought) for ML models. Rows represent the actual drought classes, while columns represent the predicted classes. Each cell shows the percentage of total samples belonging to that actual class. Diagonal cells (from top-left to bottom-right) represent correctly classified samples (true positives), while off-diagonal cells indicate misclassifications.

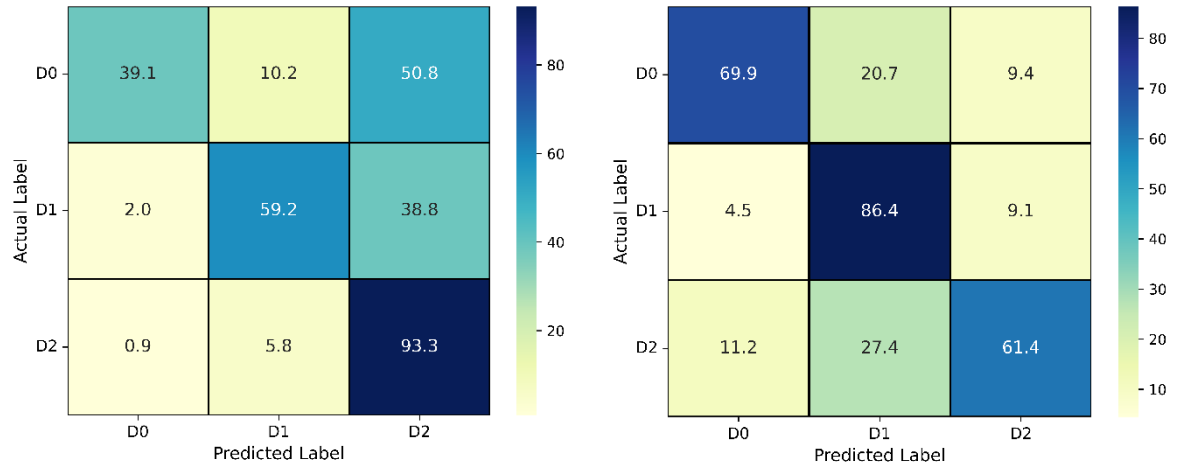

Gaussian NB

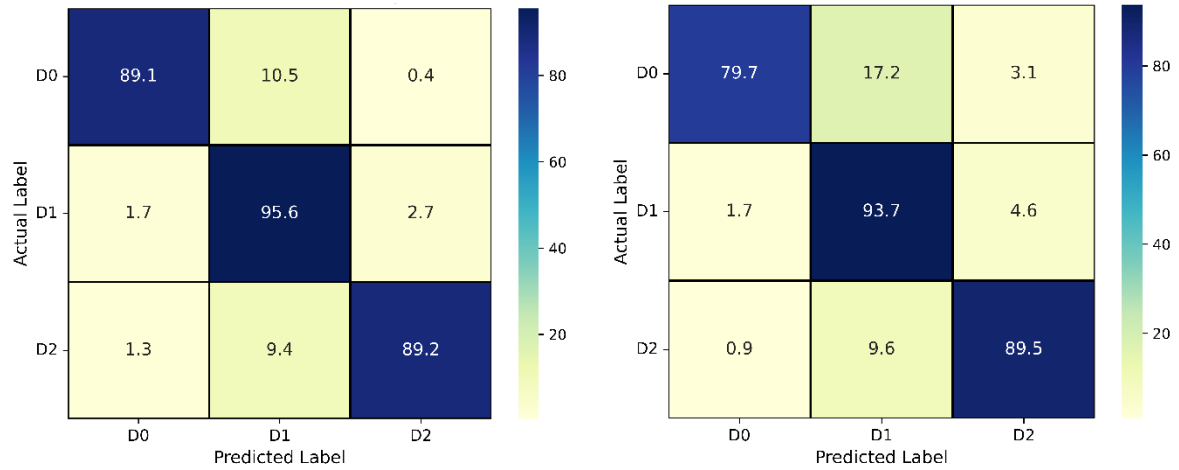

KNN

Bagging

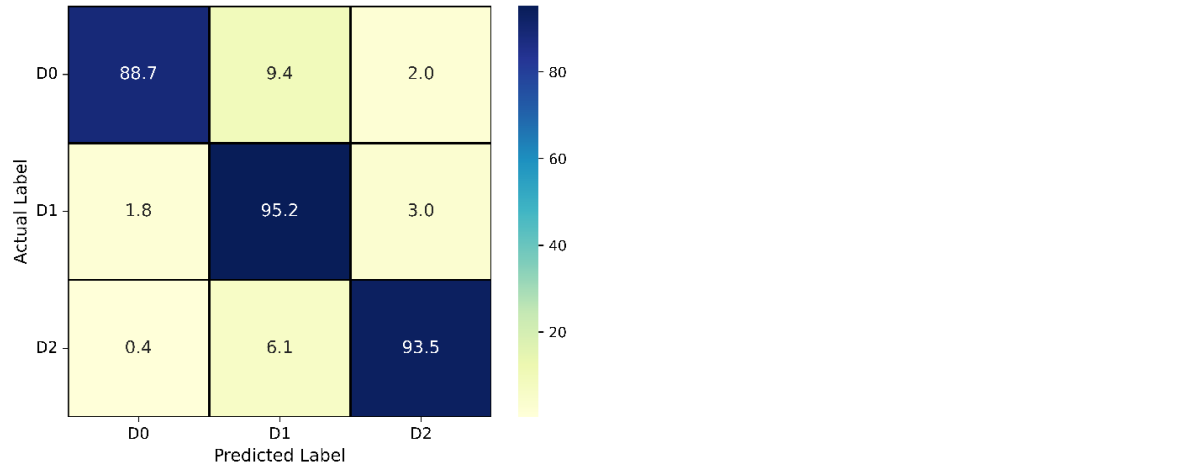

SVM

MLP

Fig.10 (continued) Confusion matrices of predicted drought classes (D0: Abnormally Dry, D1: Moderate Drought, D2: Severe Drought) for ML models. Rows represent the actual drought classes, while columns represent the predicted classes. Each cell shows the percentage of total samples belonging to that actual class. Diagonal cells (from top-left to bottom-right) represent

correctly classified samples (true positives), while off-diagonal cells indicate misclassifications.

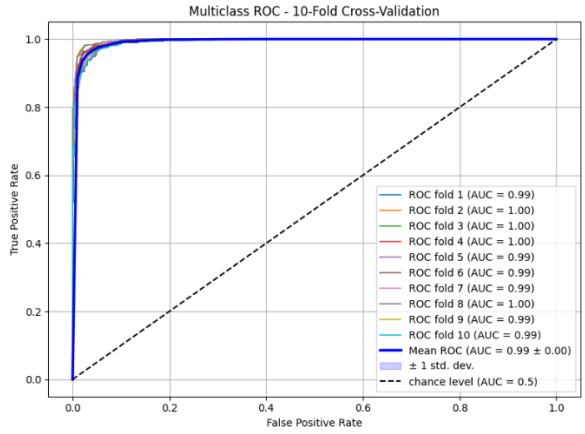

XGBRegressor

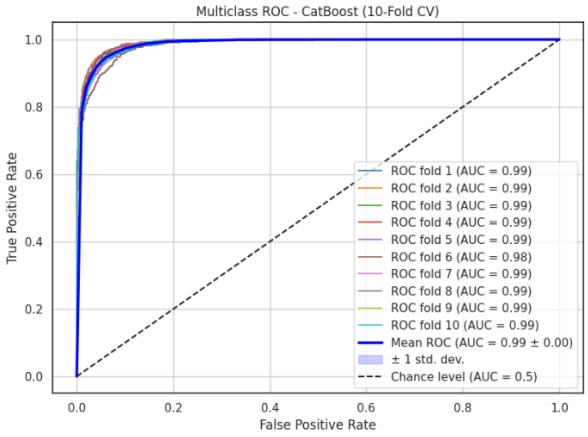

Cat Boost

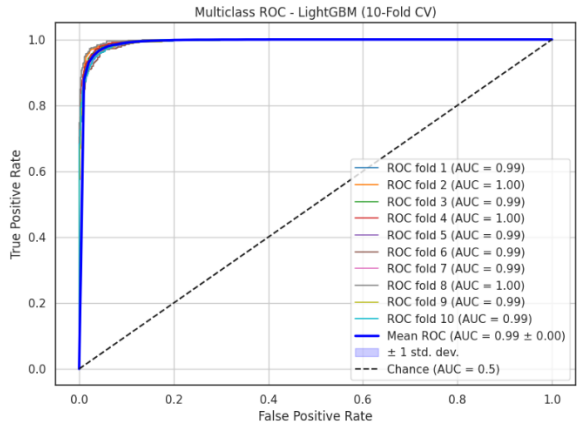

Light GBM

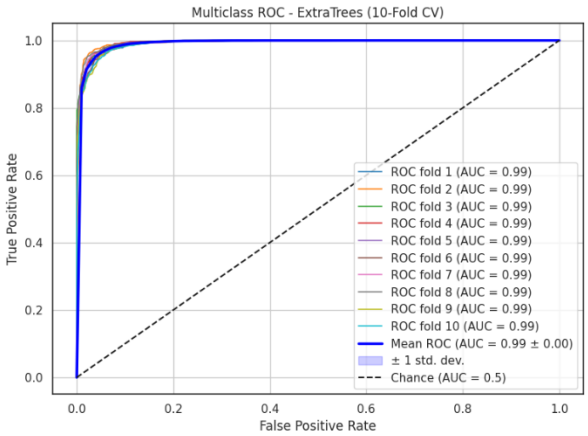

Extra Trees

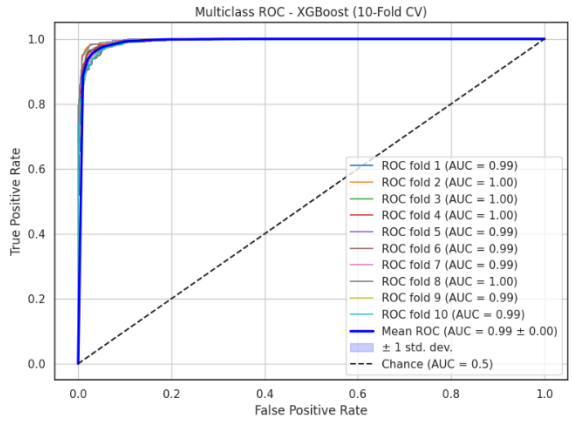

XGBoost

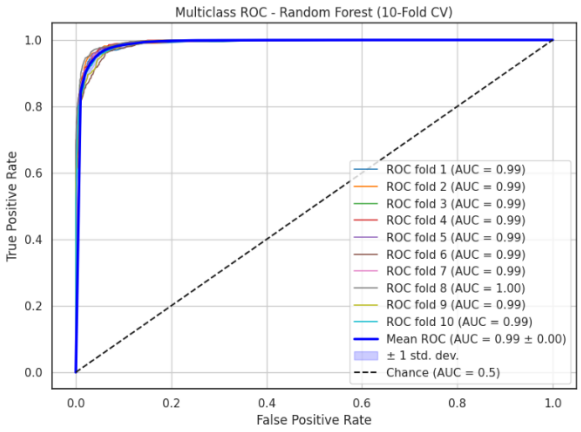

Random Forest

Fig.11 Receiver operating characteristic (ROC) curve and area under the curve (AUC) plots for each model. Here, the blue line indicates mean ROC, the grey background indicates ±1 standard deviation, the dashed line indicates chance level with AUC of 0.5, and the colored lines indicate ROC of 10 epochs.

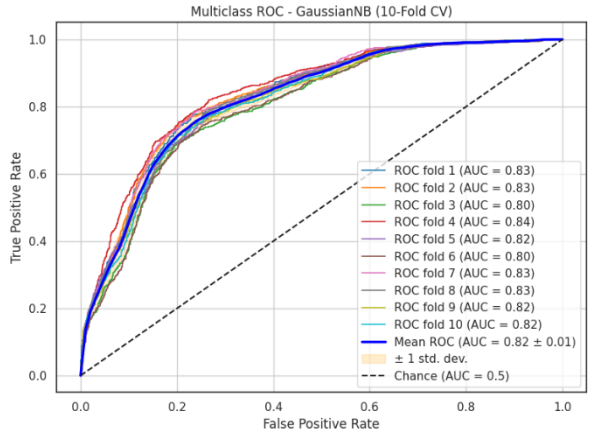

Gaussian NB

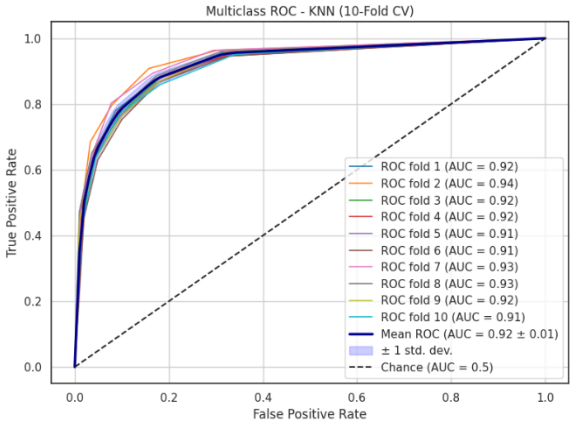

KNN

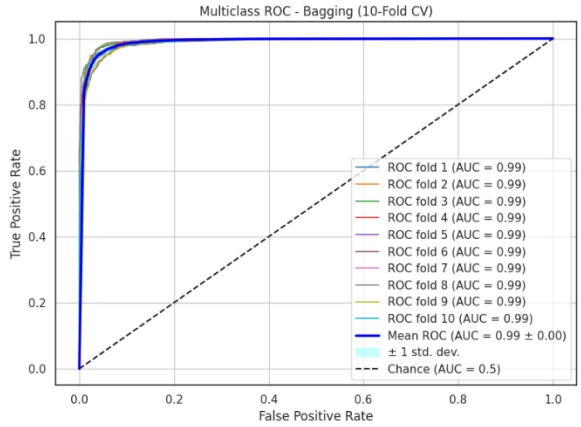

Bagging

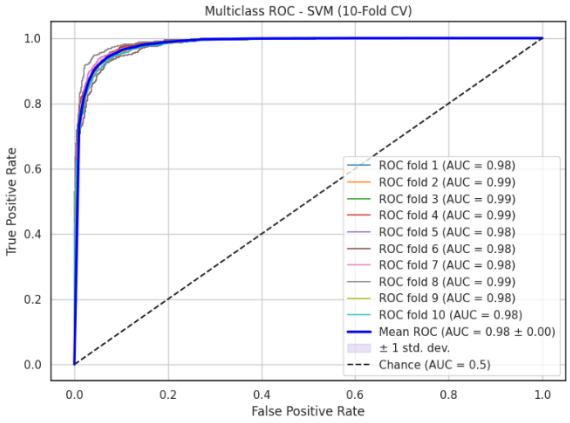

SVM

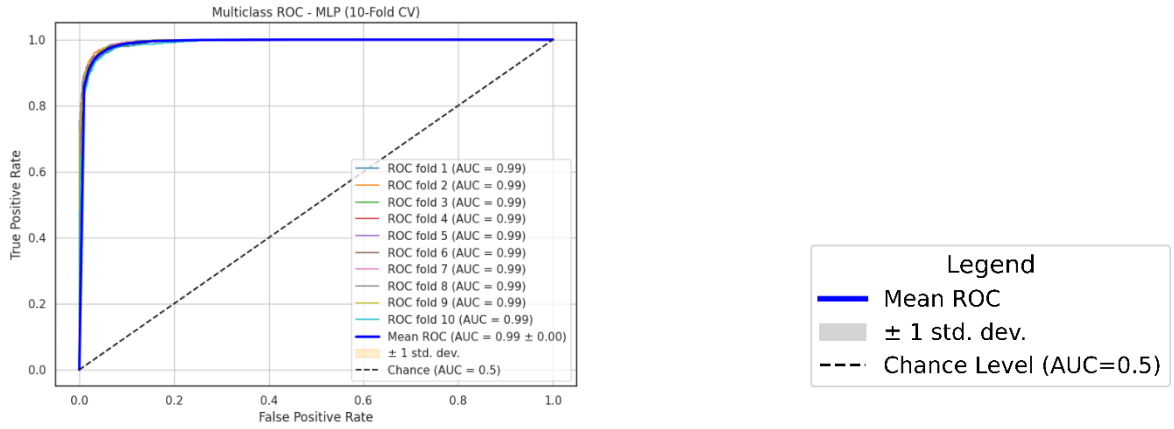

MLP

Fig.11 Receiver operating characteristic (ROC) curve and area under the curve (AUC) plots for each model. Here, the blue line indicates mean ROC, the grey background indicates ±1 standard deviation, the dashed line indicates chance level with AUC of 0.5, and the colored lines indicate ROC of 10 epochs.

4.3 Dominating Factors Controlling Drought Susceptibility

To interrogate the internal logic of high-performing classifiers, SHAP values were derived for LightGBM and XGBoost (**Figure 12**). Cumulative rainfall and surface moisture metrics emerged as dominant predictors, with rainfall deficits driving sharp positive SHAP contributions toward D1 and D2. Vegetation indices, particularly NDVI, were consistently ranked as secondary but crucial determinants. Low NDVI values were strongly associated with D2 predictions, reflecting vegetation stress as a lagged biophysical response to hydrological deficits. Conversely, elevated NDVI tended to shift classifications toward D0, signaling ecological buffering during mild anomalies.

Importantly, SHAP force plots revealed synergistic feature interactions: combinations of elevated temperatures, depressed NDVI, and reduced rainfall markedly increased the likelihood of severe drought classification. Such tri-variable coupling mirrors well-documented drought propagation pathways in the U.S. Midwest, where thermal amplification accelerates soil moisture depletion and vegetation decline (Anderson et al., 2023). Static variables such as elevation and land cover contributed minimally, serving largely as contextual background. These interpretability outputs strengthen confidence in model reasoning, aligning with broader

calls for hydrologically grounded AI in operational drought monitoring (Wang et al., 2025; Zhao et al., 2022).

4.4 Spatial Patterning of Drought Susceptibility

Geospatial outputs from the classifiers (**Figure 13**) revealed coherent patterns consistent with known regional climatology. Severe drought (D2) classifications concentrated in southern and southwestern Iowa, areas historically prone to reduced precipitation and elevated evapotranspiration. In contrast, D0 predictions clustered in northern and riverine corridors, where hydrological buffering and vegetative stability mitigate drought onset. Moderate drought (D1) was most prominent in transitional ecotones, reflecting classifiers' sensitivity to mixed hydroclimatic signals.

Topographic influences, while minor in SHAP rankings, manifested spatially. Low-lying floodplains were disproportionately associated with D2 predictions, likely due to drainage limitations and thermal accumulation, while elevated terrains demonstrated lower drought susceptibility, possibly reflecting residual soil moisture buffering from orographic precipitation. The spatial coherence across models underscores their ability to encode meaningful process–landscape interactions, a prerequisite for operational integration into localized drought risk management and water allocation planning (Teutschbein et al., 2025).

4.5 Optimal model deployment

While several ensemble models performed comparably, LightGBM emerged as the most suitable for operational deployment. Its superior macro F1 (0.94), low false-positive rate for D0, and balanced inter-class sensitivity make it particularly well-suited for early warning. Computational advantages—including histogram-based optimization, efficient memory usage, and compatibility with categorical data—further recommend its integration into near-real-time drought monitoring infrastructures. Moreover, its seamless integration with SHAP interpretability frameworks ensures transparency for decision-makers, bridging the gap between algorithmic outputs and policy utility. Although XGBoost and CatBoost achieved comparable predictive scores, their higher computational burden and reduced class stability for minority categories reduce their practicality for operational monitoring at scale.

5. Discussions

5.1 Contributions and Theoretical Implications

This study makes several contributions to the evolving field of drought monitoring through machine learning. First, it provides one of the most comprehensive benchmarks of eleven supervised algorithms across tri-class drought categories (D0–D2), directly anchored to the U.S. Drought Monitor framework. In doing so, the analysis demonstrates the operational relevance of gradient boosting architectures particularly LightGBM as classifiers capable of balancing predictive accuracy across both majority and minority drought classes. This result advances the broader discourse on AI-driven hazard modeling, where the challenge of class imbalance has historically undermined the reliability of statistical baselines such as logistic regression or Gaussian Naïve Bayes (Halder et al., 2024; Li et al., 2025).

Second, the integration of SHAP interpretability strengthens the credibility of model outputs by exposing their hydrological reasoning pathways. The identification of rainfall deficits, surface moisture anomalies, and NDVI depressions as dominant predictors not only accords with established drought process theory (Anderson et al., 2023) but also demonstrates how machine learning can recover causal-like relationships embedded in heterogeneous environmental datasets. The finding that synergistic interactions—high temperature coupled with rainfall deficit and vegetation stress—are associated with D2 predictions suggests that the models capture nonlinear relationships similar to those identified in process-based drought models (Zhao et al., 2022). This outcome responds to recent critiques that black-box machine learning, absent interpretability, risks epistemic opacity and limited policy relevance in climate-water governance (Wang et al., 2025).

Third, the geospatial consistency of model predictions demonstrates that classifiers can reproduce drought susceptibility gradients that correspond to well-documented climatic regimes in Iowa, including heightened vulnerability in the southwest and resilience in northern riverine corridors. Such coherence suggests that high-performing models are not only numerically accurate but also spatially meaningful, thereby providing a methodological bridge between data-driven approaches and landscape-process theory (Teutschbein et al., 2025). This dual accuracy and spatial fidelity strengthens the argument for integrating interpretable ML into hydroclimatic research paradigms, where both predictive fidelity and explanatory plausibility are prerequisites for advancing theory.

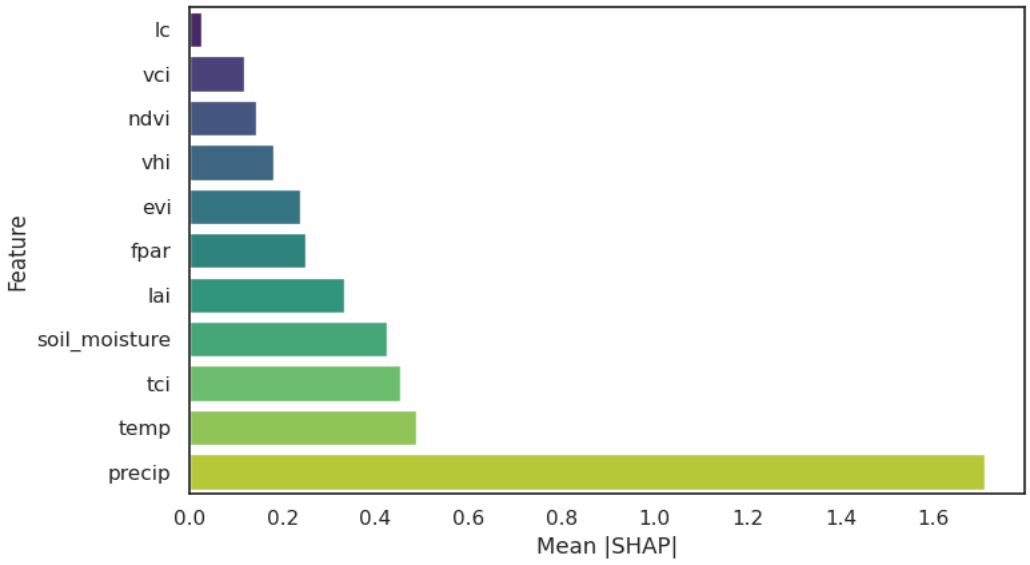

(a) Class DO

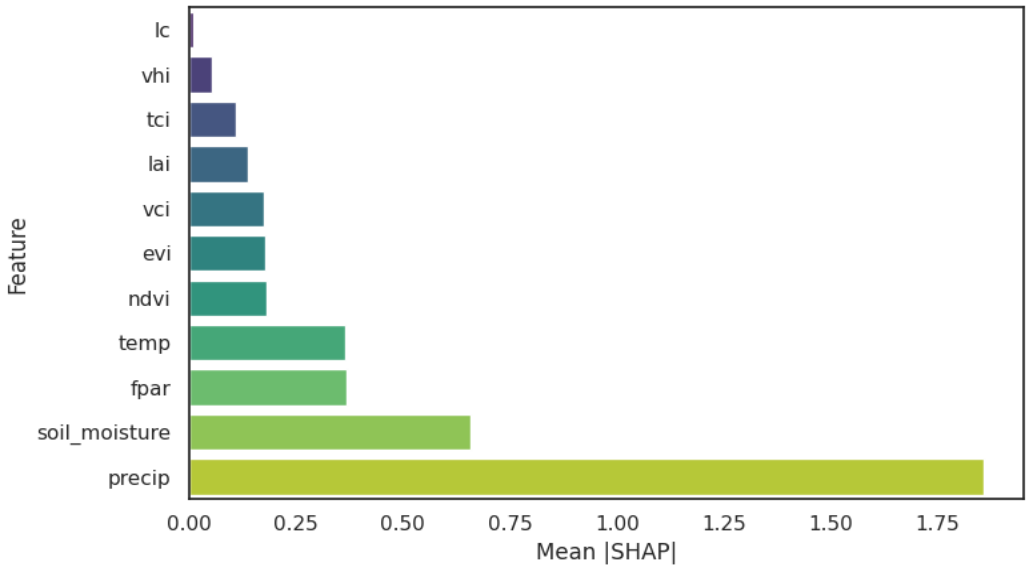

(b) Class D1

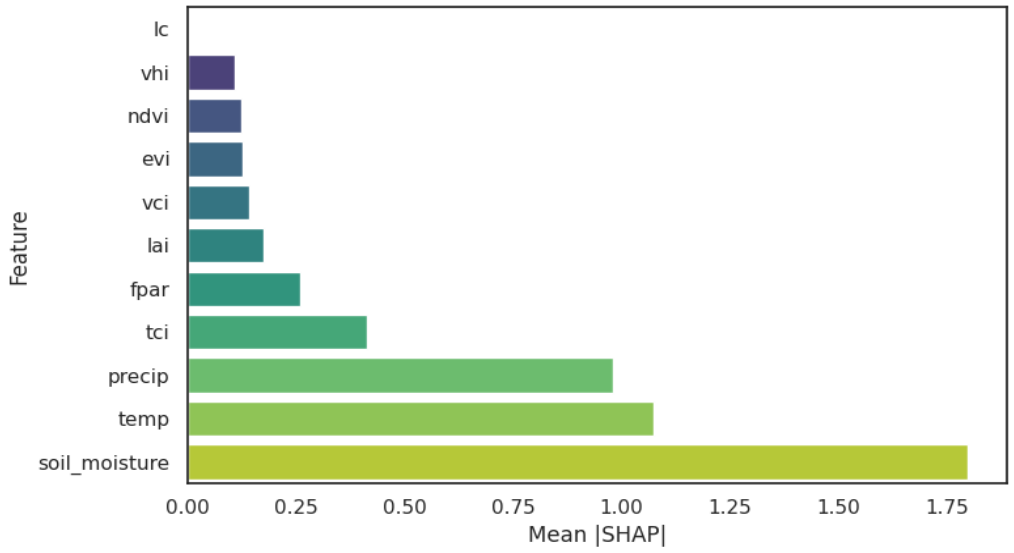

(c) Class D2

Fig.12 Mean absolute SHAP values showing the contribution of each input feature to the classification of drought by the LightGBM model.

XGB REGRESSOR

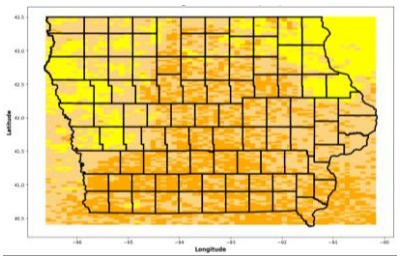

CATBOOST

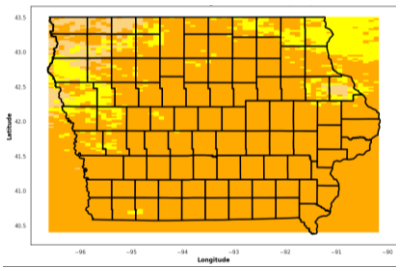

LIGHT GBM

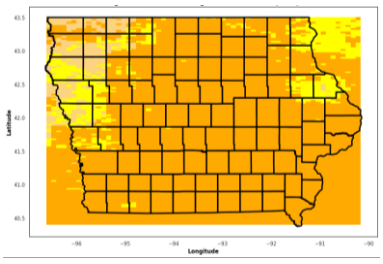

EXTRA TREES

XGBOOST

RANDOM FOREST

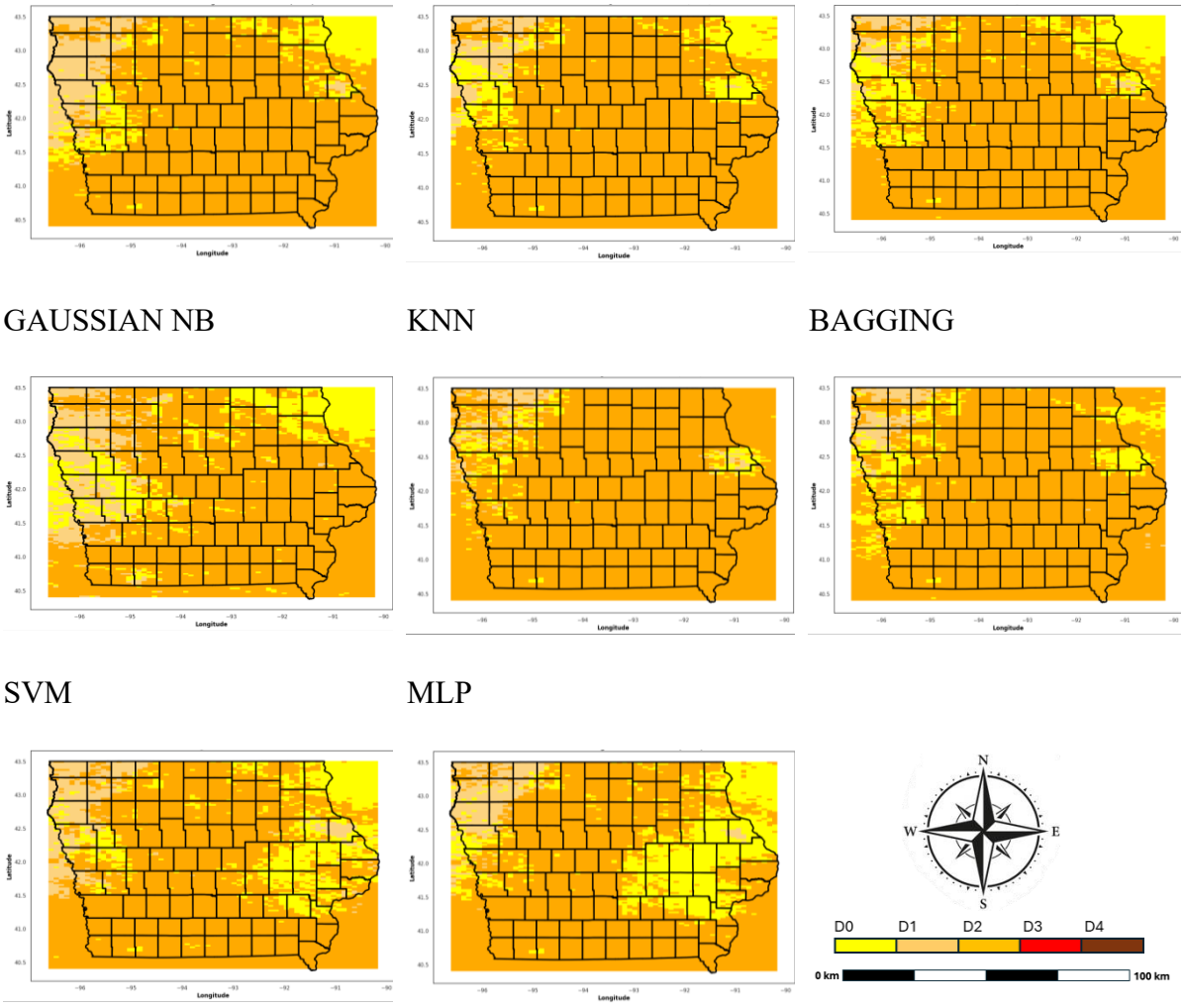

Fig.13 Geospatial classification outputs from eleven machine learning algorithms, showing predicted drought severity levels (D0 to D2) across the study region. Each panel corresponds to a distinct model, with consistent drought class labeling to facilitate inter-model comparison.

5.2 Limitations and Future Research

Despite these advances, several limitations warrant careful consideration. First, the models were trained on static historical composites, which limits their ability to anticipate drought under nonstationary climate regimes. This constraint is particularly salient given projected increases in precipitation variability and evapotranspiration demand across the Midwest. Future work should adopt temporally dynamic features—such as lagged vegetation indices,

rolling precipitation anomalies, or soil moisture persistence metrics—to better capture drought onset, propagation, and recovery cycles (Panwar et al., 2025).

Second, while SHAP provided valuable post hoc interpretability, its explanations remain correlational rather than causal. To enhance robustness, future research should explore hybrid approaches that integrate physical drought models with machine learning classifiers, or leverage causal inference frameworks capable of disentangling spurious correlations. Such integration would yield models that are both transparent and physically defensible, advancing beyond statistical mimicry toward process-informed AI (Amiri et al., 2024).

Third, model transferability across regions remains untested. Iowa's hydroclimatic regime is distinct, with agricultural dominance, riverine corridors, and humid continental climate patterns shaping drought dynamics. Application to semi-arid or monsoon-driven contexts would likely require domain adaptation, feature recalibration, or fine-tuning to account for divergent predictor distributions. Cross-regional benchmarking should therefore be prioritized to validate the generalizability of LightGBM and related algorithms.

Finally, classification of the D0 category remains the most uncertain. This reflects the inherent challenge of detecting subtle anomalies that mark the boundary between normal and abnormally dry conditions. Overcoming this weakness may require fusing multispectral satellite indices with higher-frequency meteorological data, or deploying novel sensors capable of resolving early-stage soil moisture stress.

Collectively, these limitations underscore the need for a next generation of drought monitoring frameworks that combine high-frequency Earth observations, interpretable AI, and regionally adaptive training strategies. Such efforts will ensure that machine learning advances are not only scientifically rigorous but also operationally transformative in supporting the U.S. Drought Monitor and broader climate adaptation planning.

6. Conclusion

This study demonstrates the transformative potential of machine learning and explainable artificial intelligence for drought susceptibility mapping and climate risk assessment. Through comprehensive evaluation of eleven algorithms across multiple performance metrics, we established that gradient boosting methods, particularly LightGBM, provide superior

predictive accuracy while maintaining computational efficiency and interpretability—critical requirements for operational deployment in agricultural decision-making systems.

The integration of SHAP interpretability analysis represents a significant advancement in climate informatics, bridging the gap between algorithmic performance and scientific understanding. By revealing that precipitation deficits, soil moisture anomalies, and vegetation stress indices serve as primary drought predictors, our framework validates established hydroclimatic theory while uncovering complex nonlinear interactions that traditional statistical approaches often miss. The identification of synergistic effects between temperature elevation and rainfall reduction provides mechanistic insights into drought intensification processes, contributing to fundamental understanding of hydroclimatic extremes.

From a methodological perspective, our approach addresses two persistent challenges in environmental machine learning: the black-box problem and the need for robust cross-validation in imbalanced datasets. The SHAP-based explanations ensure model transparency, while our stratified sampling and macro-averaged evaluation metrics provide reliable performance estimates across minority drought classes—a critical consideration for early warning applications where false negatives carry substantial societal costs.

The spatial coherence of our predictions with known climatological patterns strengthens confidence in model generalizability and supports the framework's potential for operational integration. The demonstrated ability to replicate United States Drought Monitor classifications while providing sub-county resolution mapping offers significant value for precision agriculture, water resource management, and climate adaptation planning.

Looking forward, this research contributes to a foundation for next-generation drought monitoring systems that combine the predictive power of modern machine learning with the interpretability demands of scientific research and policy applications. The transferable nature of our methodology suggests broad applicability to other drought-prone regions worldwide, supporting global efforts to enhance climate resilience and food security under changing environmental conditions.

Future research directions should focus on incorporating temporal dynamics through sequence modeling, expanding to multi-regional validation, and integrating additional Earth observation

datasets as they become available. The continued evolution of explainable AI techniques will further strengthen the scientific credibility and operational utility of machine learning approaches in climate and environmental sciences.

Ethics approval

Not applicable.

Consent to participate

Not applicable.

Consent for publication

Not applicable.

Competing interests

The authors declare no competing interests.

Data Availability

The datasets used and/or analyzed during the current study are available from the corresponding author on reasonable request.

Acknowledgements

This work was supported by the USDA National Institute of Food and Agriculture (Award No. 2019-67021-29227) for developing the I-Canopy platform through the project An Integrated and Smart System for Irrigation Management in Rural Communities (2019-2023). Part of the work was also supported by Public-Private Partnership (P3) funds from the University of Iowa and d by the National Science Foundation EPSCoR (Award No. 2420405) through the project Data-Advanced Research and Education (DARE) (2024-2027).

Authors contributions

Mirza Md Tasnim Mukarram: Conceptualization, Project administration, Data collection, Formal analysis, Data curation, Supervision, Resources, Software, Methodology, Investigation, Writing – original draft, Validation, Writing – review & editing.

Quazi Umme Rukiya: Project administration, Data collection, Formal analysis, Data curation, Supervision, Resources, Software, Methodology, Investigation, Writing – original draft, Validation, Writing – review & editing.

Marc Linderman: Project administration, Data collection, Formal analysis, Data curation, Supervision, Resources, Funding, Investigation, Validation, Writing – review & editing.

Jun Wang: Formal analysis, Data curation, Supervision, Resources, Software, Methodology, Investigation, Writing – original draft, Validation, Writing – review & editing.

REFERENCES

1. Seo, K. W., Ryu, D., Jeon, T., Youm, K., Kim, J. S., Oh, E. H., ... & Wilson, C. R. (2025). Abrupt sea level rise and Earth's gradual pole shift reveal permanent hydrological regime changes in the 21st century. Science, 387(6741), 1408-1413.

2. Pande, C. B., Sidek, L. M., Varade, A. M., Elkhrachy, I., Radwan, N., Tolche, A. D., & Elbeltagi, A. (2024). Forecasting of meteorological drought using ensemble and machine learning models. Environmental Sciences Europe, 36(1), 160.

3. Panwar, V., Noy, I., & Wilkinson, E. (2025). Calculating loss and damage from extreme weather events in Small Island Developing States. Regional Environmental Change, 25(2), 73.

4. Teutschbein, C., Grabs, T., Giese, M., Todorović, A., & Barthel, R. (2025). Drought propagation in high-latitude catchments: insights from a 60-year analysis using standardized indices. Natural Hazards and Earth System Sciences, 25(7), 2541-2564.

5. Zhang, L., Liu, Y., Li, Y., Ren, L., Jiang, S., Wang, M., & Wei, L. (2025). The role of precipitation deficit and potential evapotranspiration excess in triggering flash droughts over China. Journal of Hydrology, 133413.

6. Burka, A., Biazin, B., & Bewket, W. (2024). Drought susceptibility modeling with geospatial techniques and AHP model: a case of Bilate River Watershed, Central Rift Valley of Ethiopia. Geocarto International, 39(1), 2395319.

7. Gazol, A., Pizarro, M., Hammond, W. M., Allen, C. D., & Camarero, J. J. (2025). Droughts preceding tree mortality events have increased in duration and intensity, especially in dry biomes. Nature Communications, 16(1), 5779.

8. Yuan, X., Wang, Y., Ji, P., Wu, P., Sheffield, J., & Otkin, J. A. (2023). A global transition to flash droughts under climate change. Science, 380(6641), 187-191.

9. Gebrechorkos, S. H., Sheffield, J., Vicente-Serrano, S. M., Funk, C., Miralles, D. G., Peng, J., ... & Dadson, S. J. (2025). Warming accelerates global drought severity. Nature, 1-8.

10. Mishra, A., Delk, J., Mishra, A., & Zilberman, D. (2025). Drought has varying impacts on the national economy. Stochastic Environmental Research and Risk Assessment, 39(3), 925-936.

11. Douris, J., & Kim, G. (2021). The atlas of mortality and economic losses from weather, climate and water extremes (1970-2019).

12. NOAA National Centers for Environmental Information (NCEI). (2021). US billion-dollar weather and climate disasters.

13. World Meteorological Association. (2021). WMO atlas of mortality and economic losses from weather, climate and water extremes (1970–2019). WMO Rep, 90.

14. WHO (2021) Drought overview. WHO website. https://www.who.int/ health-topics/drought#

15. Ali, T., Rehman, S. U., Ali, S., Mahmood, K., Obregon, S. A., Iglesias, R. C., ... & Ashraf, I. (2024). Smart agriculture: utilizing machine learning and deep learning for drought stress identification in crops. Scientific Reports, 14(1), 30062.

16. Cos, J., Doblas-Reyes, F., Jury, M., Marcos, R., Bretonnière, P. A., & Samsó, M. (2022). The Mediterranean climate change hotspot in the CMIP5 and CMIP6 projections. Earth System Dynamics, 13(1), 321-340.

17. Yeşilköy, S., & Şaylan, L. (2022). Spatial and temporal drought projections of northwestern Turkey. Theoretical and Applied Climatology, 149(1-2), 1-14. https://doi.org/10.1007/s00704-022-04029-0

18. Leeper, R. D., Bilotta, R., Petersen, B., Stiles, C. J., Heim, R., Fuchs, B., ... & Ansari, S. (2022). Characterizing US drought over the past 20 years using the US drought monitor. International Journal of Climatology, 42(12), 6616-6630.

19. Zhang, L., Rubin, H., Chien, R. Y., Fu, J. S., Rastogi, D., Kao, S. C., & Ashfaq, M. (2025). Projected Evolution of Droughts and Human Exposure in the Contiguous United States under SSP5-8.5: A Regional Downscaling Perspective. Environmental Research Letters.

20. Smith A B 2020 U.S. Billion-dollar Weather and Climate Disasters, 1980 - present (NCEI Accession 0209268) Online: https://www.ncei.noaa.gov/archive/accession/0209268

21. Trott, C. D. (2025). Rewriting the climate story with young climate justice activists. Geographical Research, 63(1), 134-152.

22. Twumasi, Y., Merem, E. C., Fageir, S., Olagbegi, D., Wesley, J., Coney, R., ... & Emeakpor, S. (2024). Evaluating Climate Change Hazards within the US Midwest Zone. Evaluating Climate Change Hazards within the US Midwest Zone.

23. Islam, S. S., Yeşilköy, S., Baydaroğlu, Ö., Yıldırım, E., & Demir, I. (2025). State-level multidimensional agricultural drought susceptibility and risk assessment for agriculturally prominent areas. International Journal of River Basin Management, 23(2), 337-354.

24. Das, P. K., Das, K., Pandey, S. B., Das, R., Guha, A., & Pathak, S. (2025). Analysing agricultural drought resilience over Indian mainland at sub-basin level using long-term (2002-23) precipitation, soil moisture and ancillary datasets. Natural Hazards, 1-28.

25. Hoell, A., Ford, T. W., Woloszyn, M., Otkin, J. A., & Eischeid, J. (2021). Characteristics and predictability of midwestern United States drought. Journal of Hydrometeorology, 22(11), 3087-3105.

26. Bolan, S., Sharma, S., Mukherjee, S., Isaza, D. F. G., Rodgers, E. M., Zhou, P., ... & Bolan, N. (2025). Wildfires under changing climate, and their environmental and health impacts. Journal of soils and sediments, 1-25.

27. Kotz, M., Levermann, A., & Wenz, L. (2024). The economic commitment of climate change. Nature, 628(8008), 551-557.

28. Altman, J., Fibich, P., Trotsiuk, V., & Altmanova, N. (2024). Global pattern of forest disturbances and its shift under climate change. Science of the total environment, 915, 170117.

29. Liu, J., Li, M., Li, R., Shalamzari, M. J., Ren, Y., & Silakhori, E. (2025). Comprehensive assessment of drought susceptibility using predictive modeling, climate change projections, and land use dynamics for sustainable management. Land, 14(2), 337.

30. Zhou, R., Arabameri, A., Santosh, M., Islam, A. R. M. T., & Jion, M. M. M. F. (2025). Drought susceptibility prediction using novel hybridized methods based on reliability of drought and non-drought samples. Physics and Chemistry of the Earth, Parts A/B/C, 139, 103940.

31. Pulwarty, R. S., & Sivakumar, M. V. (2014). Information systems in a changing climate: Early warnings and drought risk management. Weather and Climate Extremes, 3, 14-21.

32. Haigh, T., Takle, E., Andresen, J., Widhalm, M., Carlton, J. S., & Angel, J. (2015). Mapping the decision points and climate information use of agricultural producers across the US Corn Belt. Climate Risk Management, 7, 20-30.

33. Mullapudi, A., Vibhute, A. D., Mali, S., & Patil, C. H. (2023). A review of agricultural drought assessment with remote sensing data: Methods, issues, challenges and opportunities. Applied Geomatics, 15(1), 1-13.

34. Keyantash, J. (2021). Indices for meteorological and hydrological drought. In Hydrological aspects of climate change (pp. 215-235). Singapore: Springer Singapore.

35. Edossa, D. C., Woyessa, Y. E., & Welderufael, W. A. (2016). Spatiotemporal analysis of droughts using self-calibrating Palmer's Drought Severity Index in the central region of South Africa. Theoretical and applied climatology, 126(3), 643-657.

36. Adnan, R. M., Dai, H. L., Kuriqi, A., Kisi, O., & Zounemat-Kermani, M. (2023). Improving drought modeling based on new heuristic machine learning methods. Ain Shams Engineering Journal, 14(10), 102168.

37. Deo, R. C., Byun, H. R., Adamowski, J. F., & Begum, K. (2017). Application of effective drought index for quantification of meteorological drought events: a case study in Australia. Theoretical and Applied Climatology, 128(1), 359-379.

38. Jahangir, M. H., Zarfeshani, A., & Danehkar, S. (2024). Numerical comparison of streamflow drought index (SDI) and standardized streamflow index (SSI) for evaluation of Isfahan drought status. Geology, Ecology, and Landscapes, 1-14.

39. Yuce, M. I., Deger, I. H., & Esit, M. (2023). Hydrological drought analysis of Yeşilırmak Basin of Turkey by streamflow drought index (SDI) and innovative trend analysis (ITA). Theoretical and Applied Climatology, 153(3-4), 1439-1462.

40. Katipoğlu, O. M. (2023). Prediction of streamflow drought index for short-term hydrological drought in the semi-arid Yesilirmak Basin using Wavelet transform and artificial intelligence techniques. Sustainability, 15(2), 1109.

41. Ahmadi, F., Mehdizadeh, S., & Mohammadi, B. (2021). Development of bio-inspired- and wavelet-based hybrid models for reconnaissance drought index modeling. Water Resources Management, 35(12), 4127-4147.

42. Azadeh Ranjbar, S., Kholghi, M., & Abdeh Kolahchi, A. (2025). Assessment and Validation of GRACE Satellite Data with Groundwater Resources Index (GRI) at Qazvin Aquifer Plain. Iranian Journal of Soil and Water Research, 56(4), 1103-1117.

43. Sellathurai, T., & Sivakumar, S. S. (2021). Agricultural Standardized Precipitation Index (aSPI) in Drought Characterization: A Case Study in Jaffna Peninsula in Sri Lanka.

44. Tigkas, D., Vangelis, H., Proutsos, N., & Tsakiris, G. (2022). Incorporating aSPI and eRDI in drought indices calculator (DrinC) software for agricultural drought characterisation and monitoring. Hydrology, 9(6), 100.

45. Zarei, A. R., Shabani, A., & Moghimi, M. M. (2021). Accuracy assessment of the SPEI, RDI and SPI drought indices in regions of Iran with different climate conditions. Pure and Applied Geophysics, 178(4), 1387-1403.

46. Merabti, A., Darouich, H., Paredes, P., Meddi, M., & Pereira, L. S. (2023). Assessing spatial variability and trends of droughts in eastern Algeria using SPI, RDI, PDSI, and MedPDSI—a novel drought index using the FAO56 evapotranspiration method. Water, 15(4), 626.

47. Patel, R., & Patel, A. (2024). Evaluating the impact of climate change on drought risk in semi-arid region using GIS technique. Results in Engineering, 21, 101957.

48. Nabiollahi, K., Kebonye, N. M., Molani, F., Tahari-Mehrjardi, M. H., Taghizadeh-Mehrjardi, R., Shokati, H., & Scholten, T. (2024). Assessment of Land Suitability Potential Using Ensemble Approaches of Advanced Multi-Criteria Decision Models and Machine Learning for Wheat Cultivation. Remote Sensing, 16(14).

49. Abdekareem, M., Al-Arifi, N., Abdalla, F., Mansour, A., & El-Baz, F. (2022). Fusion of remote sensing data using GIS-based AHP-weighted overlay techniques for groundwater sustainability in arid regions. Sustainability, 14(13), 7871.

50. Alsafadi, K., Bi, S., Bashir, B., Hagras, A., Alatrach, B., Harsanyi, E., ... & Mohammed, S. (2022). Land suitability evaluation for citrus cultivation (Citrus ssp.) in the southwestern Egyptian delta: a GIS technique-based geospatial MCE-AHP framework. Arabian Journal of Geosciences, 15(3), 307.

51. Ahady, A. B., Klopries, E. M., Schüttrumpf, H., & Wolf, S. (2023). Drought Analysis Methods: A Multidisciplinary Review with Insights on Key Decision-Making Factors in Method Selection. Environ. Monit. Assess, 195, 800.

52. Zhang, X., Wu, Z., Wang, H., He, C., Zhang, F., & Zhou, Y. (2024). Urban meteorological drought comprehensive index based on a composite fuzzy matter element-moment estimation weighting model. Iscience, 27(9).

53. Brust, C., Kimball, J. S., Maneta, M. P., Jencso, K., & Reichle, R. H. (2021). DroughtCast: A machine learning forecast of the United States drought monitor. Frontiers in big Data, 4, 773478.

54. Lalika, C., Mujahid, A. U. H., James, M., & Lalika, M. C. (2024). Machine learning algorithms for the prediction of drought conditions in the Wami River sub-catchment, Tanzania. Journal of Hydrology: Regional Studies, 53, 101794.

55. Piri, J., Abdolahipour, M., & Keshtegar, B. (2023). Advanced machine learning model for prediction of drought indices using hybrid SVR-RSM. Water Resources Management, 37(2), 683-712.

56. Danandeh Mehr, A., Rikhtehgar Ghiasi, A., Yaseen, Z. M., Sorman, A. U., & Abualigah, L. (2023). A novel intelligent deep learning predictive model for meteorological drought forecasting. Journal of Ambient Intelligence and Humanized Computing, 14(8), 10441-10455.

57. Prodhan, F. A., Zhang, J., Hasan, S. S., Sharma, T. P. P., & Mohana, H. P. (2022). A review of machine learning methods for drought hazard monitoring and forecasting: Current research trends, challenges, and future research directions. Environmental modelling & software, 149, 105327.

58. Xu, X., Chen, F., Wang, B., Harrison, M. T., Chen, Y., Liu, K., ... & Hu, K. (2024). Unleashing the power of machine learning and remote sensing for robust seasonal drought monitoring: A stacking ensemble approach. Journal of Hydrology, 634, 131102.

59. Al Mamun, M. A., Sarker, M. R., Sarkar, M. A. R., Roy, S. K., Nihad, S. A. I., McKenzie, A. M., ... & Kabir, M. S. (2024). Identification of influential weather parameters and seasonal drought prediction in Bangladesh using machine learning algorithm. Scientific reports, 14(1), 566.

60. Abdel-Fattah, M. K., Mokhtar, A., & Abdo, A. I. (2021). Application of neural network and time series modeling to study the suitability of drain water quality for irrigation: a case study from Egypt. Environmental Science and Pollution Research, 28(1), 898-914.

61. Mokhtar, A., Jalali, M., He, H., Al-Ansari, N., Elbeltagi, A., Alsafadi, K., ... & Rodrigo-Comino, J. (2021). Estimation of SPEI meteorological drought using machine learning algorithms. IEEe Access, 9, 65503-65523.

62. Zhang, R., Chen, Z. Y., Xu, L. J., & Ou, C. Q. (2019). Meteorological drought forecasting based on a statistical model with machine learning techniques in Shaanxi province, China. Science of the Total Environment, 665, 338-346.

63. Hao, Z., Singh, V. P., & Xia, Y. (2018). Seasonal drought prediction: Advances, challenges, and future prospects. Reviews of Geophysics, 56(1), 108-141.

64. Pilz, T., Delgado, J. M., Voss, S., Vormoor, K., Francke, T., Costa, A. C., ... & Bronstert, A. (2019). Seasonal drought prediction for semiarid northeast Brazil: what is the added value

of a process-based hydrological model?. Hydrology and Earth System Sciences, 23(4), 1951-1971.

65. Troin, M., Arsenault, R., Wood, A. W., Brissette, F., & Martel, J. L. (2021). Generating ensemble streamflow forecasts: A review of methods and approaches over the past 40 years.

66. Granata, F. (2019). Evapotranspiration evaluation models based on machine learning algorithms—A comparative study. Agricultural Water Management, 217, 303-315.

67. Mouatadid, S., Raj, N., Deo, R. C., & Adamowski, J. F. (2018). Input selection and data-driven model performance optimization to predict the Standardized Precipitation and Evaporation Index in a drought-prone region. Atmospheric research, 212, 130-149.

68. Rolnick, D., Donti, P. L., Kaack, L. H., Kochanski, K., Lacoste, A., Sankaran, K., ... & Bengio, Y. (2022). Tackling climate change with machine learning. ACM Computing Surveys (CSUR), 55(2), 1-96.

69. Liu, X., Lu, D., Zhang, A., Liu, Q., & Jiang, G. (2022). Data-driven machine learning in environmental pollution: gains and problems. Environmental science & technology, 56(4), 2124-2133.

70. Hamdan, A., Ibekwe, K. I., Etukudoh, E. A., Umoh, A. A., & Ilojianya, V. I. (2024). AI and machine learning in climate change research: A review of predictive models and environmental impact. World Journal of Advanced Research and Reviews, 21(1), 1999-2008.

71. Kikon, A., & Deka, P. C. (2021). Forecasting of meteorological drought using machine learning algorithm. In Advanced Modelling and Innovations in Water Resources Engineering: Select Proceedings of AMIWRE 2021 (pp. 43-52). Singapore: Springer Singapore.

72. Yaseen, Z. M., Ali, M., Sharafati, A., Al-Ansari, N., & Shahid, S. (2021). Forecasting standardized precipitation index using data intelligence models: regional investigation of Bangladesh. Scientific reports, 11(1), 3435.

73. Lotfirad, M., Esmaeili-Gisavandani, H., & Adib, A. (2022). Drought monitoring and prediction using SPI, SPEI, and random forest model in various climates of Iran. Journal of Water and Climate Change, 13(2), 383-406.

74. Kisi, O., Gorgij, A. D., Zounemat-Kermani, M., Mahdavi-Meymand, A., & Kim, S. (2019). Drought forecasting using novel heuristic methods in a semi-arid environment. Journal of Hydrology, 578, 124053.

75. Masinde, M., Mwagha, M., & Tadesse, T. (2018). Downscaling africa's drought forecasts through integration of indigenous and scientific drought forecasts using fuzzy cognitive maps. Geosciences, 8(4), 135.

76. Belayneh, A., Adamowski, J., Khalil, B., & Ozga-Zielinski, B. J. J. O. H. (2014). Long-term SPI drought forecasting in the Awash River Basin in Ethiopia using wavelet neural network and wavelet support vector regression models. Journal of Hydrology, 508, 418-429.

77. Oyarzabal, R. S., Santos, L. B., Cunningham, C., Broedel, E., de Lima, G. R., Cunha-Zeri, G., ... & Cunha, A. P. (2025). Forecasting drought using machine learning: a systematic literature review. Natural Hazards, 1-29.

78. Oyounalsoud, M. S., Yilmaz, A. G., Abdallah, M., & Abdeljaber, A. (2024). Drought prediction using artificial intelligence models based on climate data and soil moisture. Scientific reports, 14(1), 19700.

79. Khan, M. I., & Maity, R. (2024). Development of a long-range hydrological drought prediction framework using deep learning. Water Resources Management, 38(4), 1497-1509.

80. Latifoğlu, L., Bayram, S., Aktürk, G., & Citakoglu, H. (2024). Drought index time series forecasting via three-in-one machine learning concept for the Euphrates basin. Earth Science Informatics, 17(6), 5841-5898.

81. Materia, S., García, L. P., van Straaten, C., O, S., Mamalakis, A., Cavicchia, L., ... & Donat, M. (2024). Artificial intelligence for climate prediction of extremes: State of the art, challenges, and future perspectives. Wiley Interdisciplinary Reviews: Climate Change, 15(6), e914.

82. Eddamiri, S., Bassine, F. Z., Hakam, O., Kambiet, P. L. K., & Chehbouni, A. (2025). Applications of artificial intelligence for forecasting and managing extremes. In Climate Change and Rainfall Extremes in Africa (pp. 91-113). Elsevier.

83. Camps-Valls, G., Fernández-Torres, M. Á., Cohrs, K. H., Höhl, A., Castelletti, A., Pacal, A., ... & Williams, T. (2025). Artificial intelligence for modeling and understanding extreme weather and climate events. Nature Communications, 16(1), 1919.

84. Brunner, M. I., Slater, L., Tallaksen, L. M., & Clark, M. (2021). Challenges in modeling and predicting floods and droughts: A review. Wiley Interdisciplinary Reviews: Water, 8(3), e1520.

85. Cappellazzo, M., Patrucco, G., Sammartano, G., Baldo, M., & Spanò, A. (2024). Semantic Mapping of Landscape Morphologies: Tuning ML/DL Classification Approaches for Airborne LiDAR Data. Remote Sensing, 16(19), 3572.

86. Pendergrass, A. G., Meehl, G. A., Pulwarty, R., Hobbins, M., Hoell, A., AghaKouchak, A., ... & Woodhouse, C. A. (2020). Flash droughts present a new challenge for subseasonal-to-seasonal prediction. Nature Climate Change, 10(3), 191-199.

87. Otkin, J. A., Svoboda, M., Hunt, E. D., Ford, T. W., Anderson, M. C., Hain, C., & Basara, J. B. (2018). Flash droughts: A review and assessment of the challenges imposed by rapid-onset droughts in the United States. Bulletin of the American Meteorological Society, 99(5), 911-919.

88. Reichstein, M., Camps-Valls, G., Stevens, B., Jung, M., Denzler, J., Carvalhais, N., & Prabhat, F. (2019). Deep learning and process understanding for data-driven Earth system science. Nature, 566(7743), 195-204.

89. Tadesse, B., & Ahmed, M. (2023). Impact of adoption of climate smart agricultural practices to minimize production risk in Ethiopia: a systematic review. J Agric Food Res 13: 100655.

90. Samek, W. (2023). Explainable deep learning: concepts, methods, and new developments. In Explainable Deep Learning AI (pp. 7-33). Academic Press.

91. Islam, S. S., Yeşilköy, S., Baydaroğlu, Ö., Yıldırım, E., & Demir, I. (2025). State-level multidimensional agricultural drought susceptibility and risk assessment for agriculturally prominent areas. International Journal of River Basin Management, 23(2), 337-354.

92. Shepard, R. C., Bitterman, P., Archer, J. C., & Shelley, F. M. (2024). Atlas of Iowa. University of Iowa Press.

93. Yang, X., & Jin, W. (2010). GIS-based spatial regression and prediction of water quality in river networks: A case study in Iowa. Journal of Environmental Management, 91(10), 1943-1951.

94. Yildirim, E., & Demir, I. (2022). Agricultural flood vulnerability assessment and risk quantification in Iowa. Science of The Total Environment, 826, 154165.

95. USDA, 2024. USDA - Iowa Ag News – Crop Production.

96. Sun, H., Upadhaya, S., Morris, C., Arbuckle, J., Nowatzke, L., & Zhu, Z. (2025). The Flux of Agricultural Conservation: Understanding Changes in Iowa Farmers' Adoption of Cover Crops and No-Till Over Time. Society & Natural Resources, 1-20.

97. Peters, K. S. (2024). Iowa Needs (Clean Energy) Farmers. Iowa L. Rev., 110, 1863.

98. Grant, C. A., Alabbad, Y., Yildirim, E., & Demir, I. (2024). Comprehensive Assessment of Flood Risk and Vulnerability for Essential Facilities: Iowa Case Study. Urban Science, 8(3), 145.

99. Hashemi, M. G., Alemohammad, H., Jalilvand, E., Tan, P. N., Judge, J., Cosh, M., & Das, N. N. (2025). Estimating crop biophysical parameters from satellite-based SAR and optical observations using self-supervised learning with geospatial foundation models. Remote Sensing of Environment, 327, 114825.

100. Federal Emergency Management Agency (FEMA), 2021. Disaster Declarations for States and Counties. https://www.fema.gov/data-visualization/disaster-declarations-states-andcounties. Accessed August 2025.

101. Cintura, I., & Arenas, A. (2025). Projection and Assessment of Future Droughts in Iowa: Developing a Machine Learning Model and an Interactive Application. Frontiers in Environmental Science, 13, 1564670.

102. NOAA National Centers for Environmental Information. (2024). Billion-dollar weather and climate disasters: Iowa. NOAA. https://www.ncei.noaa.gov/access/billions/state-summary/IA

103. Hatami Bahman Beiglou, P., Luo, L., Tan, P. N., & Pei, L. (2021). Automated analysis of the US drought monitor maps with machine learning and multiple drought indicators. Frontiers in big Data, 4, 750536.

104. Hao, Zengchao, and Amir AghaKouchak. "A nonparametric multivariate multi-index drought monitoring framework." Journal of Hydrometeorology 15.1 (2014): 89-101.

105. Feng, P., Wang, B., Li Liu, D., & Yu, Q. (2019). Machine learning-based integration of remotely-sensed drought factors can improve the estimation of agricultural drought in South-Eastern Australia. Agricultural Systems, 173, 303-316.

106. Park, S., Im, J., Jang, E., & Rhee, J. (2016). Drought assessment and monitoring through blending of multi-sensor indices using machine learning approaches for different climate regions. Agricultural and forest meteorology, 216, 157-169.

107. Hobeichi, S., Abramowitz, G., Evans, J. P., & Ukkola, A. (2022). Toward a robust, impact-based, predictive drought metric. Water Resources Research, 58(2), e2021WR031829.

108. Melese, T., Assefa, G., Terefe, B., Belay, T., Bayable, G., & Senamew, A. (2025). Machine learning-based drought prediction using Palmer Drought Severity Index and TerraClimate data in Ethiopia. PLoS One, 20(6), e0326174.

109. Ali, T., Rehman, S. U., Ali, S., Mahmood, K., Obregon, S. A., Iglesias, R. C., ... & Ashraf, I. (2024). Smart agriculture: utilizing machine learning and deep learning for drought stress identification in crops. Scientific Reports, 14(1), 30062.

110. Barradas, A., Correia, P. M., Silva, S., Mariano, P., Pires, M. C., Matos, A. R., ... & Marques da Silva, J. (2021). Comparing machine learning methods for classifying plant drought stress from leaf reflectance spectra in Arabidopsis thaliana. Applied Sciences, 11(14), 6392.

111. Zhang, B., Salem, F. K. A., Hayes, M. J., Smith, K. H., Tadesse, T., & Wardlow, B. D. (2023). Explainable machine learning for the prediction and assessment of complex drought impacts. Science of The Total Environment, 898, 165509.

112. Wang, W., Wang, Q. J., & Nathan, R. (2025). Gaussian process regression on multiple drivers and attributes for rapid prediction of maximum flood inundation extent and depth. *Journal of Hydrology*, *649*, 132476.

113. Halder, R. K., Uddin, M. N., Uddin, M. A., Aryal, S., & Khraisat, A. (2024). Enhancing K-nearest neighbor algorithm: a comprehensive review and performance analysis of modifications. *Journal of Big Data*, *11*(1), 113.

114. Glinka, S., Owerko, T., & Tomaszkiewicz, K. (2022). Using open vector-based spatial data to create semantic datasets for building segmentation for raster data. *Remote Sensing*, *14*(12), 2745.

115. Hao, Z., & Singh, V. P. (2015). Drought characterization from a multivariate perspective: A review. *Journal of Hydrology*, *527*, 668-678.

116. Ma, H., Cui, T., & Cao, L. (2023). Monitoring of drought stress in Chinese forests based on satellite solar-induced chlorophyll fluorescence and multi-source remote sensing indices. *Remote Sensing*, *15*(4), 879.

117. Li, J., Li, Y., Yin, L., & Zhao, Q. (2024). A novel composite drought index combining precipitation, temperature and evapotranspiration used for drought monitoring in the Huang-Huai-Hai Plain. *Agricultural Water Management*, *291*, 108626.

118. Du, L., Tian, Q., Yu, T., Meng, Q., Jancso, T., Udvardy, P., & Huang, Y. (2013). A comprehensive drought monitoring method integrating MODIS and TRMM data. *International Journal of Applied Earth Observation and Geoinformation*, *23*, 245-253.

119. Oyounalsoud, M. S., Yilmaz, A. G., Abdallah, M., & Abdeljaber, A. (2024). Drought prediction using artificial intelligence models based on climate data and soil moisture. *Scientific reports*, *14*(1), 19700.

120. Xiao, C., Zaehle, S., Yang, H., Wigneron, J. P., Schmullius, C., & Bastos, A. (2023). Land cover and management effects on ecosystem resistance to drought stress. *Earth System Dynamics*, *14*(6), 1211-1237.

121. Bento, V. A., Gouveia, C. M., DaCamara, C. C., & Trigo, I. F. (2018). A climatological assessment of drought impact on vegetation health index. *Agricultural and forest meteorology*, *259*, 286-295.